UNIVERSITY OF HAWAII

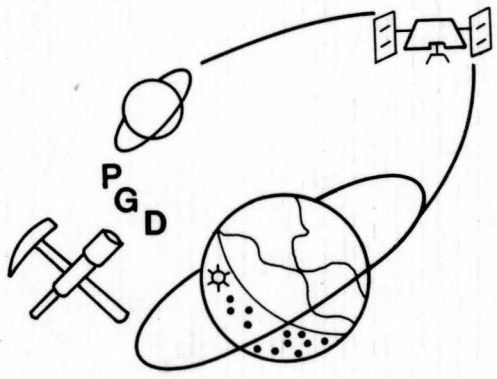

Planetary Geosciences Division

HAWAII INSTITUTE OF GEOPHYSICS

2525 CORREA ROAD • HONOLULU, HAWAII 96822

808-948-6488

Observations of Mars During the 1986 and 1988 Perihelic Oppositions: 0.4-2.5 μm Reflectance Spectroscopy of Small Surface Regions With Emphasis on Iron Oxide Minerals

by

James Francis Bell III

PGD Contribution No. 577

OBSERVATIONS OF MARS DURING THE 1986 AND 1988 PERIHELIC OPPOSITIONS: 0.4-2.5 μm REFLECTANCE SPECTROSCOPY OF SMALL SURFACE REGIONS WITH EMPHASIS ON IRON OXIDE MINERALS

A THESIS SUBMITTED TO THE GRADUATE DIVISION OF THE UNIVERSITY OF HAWAII IN PARTIAL FULFILLMENT OF THE REQUIREMENTS FOR THE DEGREE OF

MASTER OF SCIENCE

IN GEOLOGY AND GEOPHYSICS

AUGUST 1989

By

James Francis Bell, III

Thesis Committee:

Thomas B. McCord, Chairman
Fraser P. Fanale
Peter J. Mouginis-Mark
Paul G. Lucey
William M. Sinton

We certify that we have read this thesis and that, in our opinion, it is satisfactory in scope and quality as a thesis for the degree of Master of Science in Geology and Geophysics.

THESIS COMMITTEE

H. B. Kanamori

Chairman

Peter J. Mayes-Munk

Paul Lucey

Duncan Agnew

William M. Kaula

ACKNOWLEDGEMENTS

There are a great number of people without whom this research would have been impossible to carry out. First, I would like to thank the entire support staff of the University of Hawaii telescopes on Mauna Kea. These telescope operators, engineers, cooks, and secretaries perform a vital and often unheralded service to the astronomical community. The strenuous work at high altitudes is surpassed in its difficulty only by having to deal with stress-filled, oxygen-deprived, and often hard-headed astronomers and graduate students year round.

The support of the graduate students, research staff, and faculty of the Planetary Geosciences Division (PGD) has been exceptional. Above all, I would like to mention the assistance of Pam Owensby and Paul Lucey as being perhaps the most useful and instructive during my first two years here in Hawaii. Our shared experiences with telescopic equipment, observing methods, laboratory instrumentation, and data reduction have made these two fun-loving scientists not only friends, but mentors and role models. They are planetary astronomers *par excellence.*

Constantly working behind the scenes of this two year project was the able-bodied PGD administrative staff. Thank you Sam, Zeny, Diane, Donna, Ara, Janet, Jody, Michele, Lorna, and Leilani for (a) getting me there, (b) making sure my stuff got there with me, and (c) finding someone to pay for it all.

Speaking of paying for it all, I would like to thank the rest of my Thesis Committee, Fraser Fanale, Peter Mouginis-Mark, Bill Sinton, and my advisor Tom McCord for helpful insights and guidance, reviews of papers and presentations, trinkets from foreign lands, and occasional games of racquetball.

Additionally, I thank Cassandra Coombs (now at NASA/JSC) for invaluable help formatting this document (ugh! unix!), Leonard Martin (Lowell Observatory/The National Geographic Society/University of Missouri) for providing beautiful Planetary Patrol photographs of Mars during 1986 and 1988, Dick

Morris (NASA/JSC) for several helpful discussions and figures on laboratory iron oxide studies, the Caltech Summer Undergraduate Research Fellowship (SURF) faculty and staff for sponsoring this research during the summer of 1986, and Andy Ingersoll, who originally set the gears in motion for my first encounter with Mauna Kea, a place more like Mars than nearly any other place on Earth.

To my friend Bruce Campbell, thanks for the programming support and general advice on techniques of social radar-lock. Remember Goose, even if you've got good tone, you never *ever* leave your wing man.

Finally, the constant thread which has held me together through all the trepidations of stress, poverty, and personal crises in the years since I graduated from high school has been my family. To my parents, James and Angela Bell, who in July of 1965 were too busy with other matters closer to home to be aware of Mariner IV's historic flyby of Mars, thank you for all the love and support. Who could have known what it would lead to when you helped me buy my first real telescope, an 8″ Newtonian reflector, all those years ago? And to Maureen Ockert, my best friend and fianceé, thank you for the friendship, support, and love which have held me together of late. Boy, could I use one of your neckrubs right now...

ABSTRACT

This thesis represents the results of one aspect of an extensive program of telescopic observations of Mars which I carried out during the 1986 and 1988 oppositions at the Mauna Kea Observatory, Hawaii. During 1986, relative reflectance spectra were obtained for a number of small regions in the bright western hemisphere of Mars in the 0.7-2.5 μm wavelength range. During 1988, both relative reflectance and spectral reflectance data were obtained for similarly sized regions (200-600 km diameter) also in the western hemisphere in the 0.4-1.0 μm range.

The 1986 data show a consistent lack of noticeable differences between spectra taken of areas which, in geologic maps and Viking Orbiter images, appear to have very different morphologies. Of the possible interpretations of this observation, the most likely is that a grossly uniform mantle of global dust covers much of the observed surface, consistent with several previous studies based on ground-based spectral reflectance and radar observations as well as Viking Orbiter thermal inertia (particle sizes) and albedo measurements. The basic conclusion is that spectral differences are small (only a few percent of the continuum) or nonexistent among many areas on Mars on the scale of several hundred kilometers.

The 1988 spectral reflectance data (at a higher spatial and spectral resolution than any other published datasets from 0.4-1.0 μm) show several distinct Fe^{3+} absorption bands at ~0.62-0.72 and ~0.81-0.94 μm which have never before been so evident. These bands are interpreted as Fe^{3+} electronic transition features that indicate the presence of *crystalline* ferric oxide or hydroxide minerals on the martian surface. Comparison of the new data with laboratory studies of other workers supports recent conclusions that a single iron oxide phase, most likely hematite ($\alpha-Fe_2O_3$) existing in a wide range of particle sizes, could be responsible for much or all of the observed spectral behavior of the martian soils and dust in the 0.4-1.0 μm region.

TABLE OF CONTENTS

LIST OF TABLES

LIST OF FIGURES

CHAPTER 1

INTRODUCTION

My far-off goal seems strangely near,
Luring imagination on,
Beckoning body to be gone
To ruddy-earthed, blue-oceaned Mars.
—Percival Lowell, 1894

For much of the past three centuries, Mars has been an enigmatic source of intense scientific debate and public curiousity. Among the terrestrial planets, Mars was recognized by early observers such as Huygens, Cassini, Maraldi, Herschel, and Schroeter to be the most "earth-like" in its telescopic appearance. In analogy with the Moon, bright and dark regions came to be known as "lands" and "seas," and eventually the semantics became intertwined with the geologic interpretations. Inferences of these early pioneers combined with higher quality telescopes of the late nineteenth century allowed observers like Beer and Mädler, Proctor, Green, and Schiaparelli to conclude that not only did Mars have an atmosphere, but it also probably had, if not oceans, some amount of liquid water on its surface. The highly controversial claims of Schiaparelli during 1878 (based in part on observations by Father Secchi in the 1860's) concerning dark linear markings or "*canali,*" set the stage for perhaps the most heated controversy of modern-day astronomy. One camp, led by Lowell, claimed the "*canali,*" or literally interpreted, "canals," were the product of intelligent design, carried out by the desperate inhabitants of Mars trying to battle the dessication of their

planet through global irrigation. The other side, led by the observers Maunder and Antoniadi, claimed the "canals" were no more than an illusory effect caused by inadequate resolution of intricate details on the martian surface. This debate, and its implications for the evolution of life and of planets themselves, was to rage on until the dawn of the space age. The long and controversial history of Mars observations has always stirred the interest of scientist and layman alike, and is one of the reasons that detailed scientific observations of Mars using the world's great telescopes continues to this day.

When Mars and the Earth pass each other in their orbits, the event is called an "opposition." Because the orbit of Mars is rather eccentric, these oppositions occur in cycles of very close passes and very distant passes, some 15-17 years apart. The 1986 and 1988 oppositions of Mars were very close passes (~56 million km) occurring near the perihelion of the martian orbit, and are thus called perihelic oppositions. During 1986 and 1988, Mars grew to nearly 25 arcseconds in apparent diameter and remained well above the horizon for much of the midlatitudes observing season. This was an excellent time to observe Mars close-up, and would be a rare opportunity to answer some still outstanding questions. Two questions in particular drove the research reported in this thesis: First, what is the real nature of the martian surface in terms of chemical composition or mineralogy? And second, what is the real nature of the differences between the bright and the dark albedo regions observed for the past 300 years? A series of spectroscopic observations was undertaken in an attempt find answers to these questions.

Chapter 2 describes a series of observations which I made during the 1986 opposition in the 0.7-2.5 μm region using a circular variable filter (CVF) spectrometer with a resolving power R of 60-80 ($R = \lambda/\Delta\lambda$). These measurements were made in an attempt to detect mineralogic differences between various regions on the planet. Although the spectra were not photometrically

corrected using standard star observations and thus absolute mineralogies could not be inferred, the method of relative reflectance spectroscopy (flux of one area/flux of another area) was employed to determine whether conclusive morphologic differences seen between regions in the Viking Orbiter images correlated with spectral and therefore chemical or mineralogic differences. The results of this study showed that spectral differences are small or even nonexistent among many areas on Mars at the several hundred kilometer scale. Apparently, the martian global dust deposits act to reduce the spectral contrast of the surface materials, making the measurement of spectral differences even between the brightest and the darkest regions extremely difficult and very sensitive to the spatial resolution employed.

Chapter 3 details another set of comprehensive observations of Mars, this time during the 1988 opposition, which I performed using a CVF spectrophotometer in the 0.4-1.0 μm range (R = 80-100). The near-UV to near-IR spectral region is extremely sensitive to iron mineralogies, there being a whole series of Fe^{3+} and Fe^{2+} electronic transition bands in this wavelength range. Spectral reflectance data calibrated through standard solar analog stars were obtained for a number of small regions on the planet. In addition, a series of relative reflectance spectra much like those shown in Chapter 2 are presented. The relative reflectance data show slope differences at wavelengths less than 0.7 μm for many of the regions compared which may relate to ferric iron content differences between the surface soils observed. The main emphasis will be on the detection of specific, crystalline Fe^{3+} absorption bands in the spectral reflectance data which have never before been so evident in previous studies at lower spatial and spectral resolution. Variations in these bands between bright and dark regions seem to indicate a higher Fe^{3+} content in the bright region soils, consistent with the relative reflectance data which show the bright regions to be generally more red than the darker regions. These new data are then compared

with laboratory studies of ferric oxides and hydroxides by other workers. The conclusion is then reached, in support of other interpretations discussed in the text, that crystalline hematite ($\alpha-Fe_2O_3$) has been detected on the surface of Mars. This finding is found to be consistent with measurements made on the martian surface by the Viking Landers (which unfortunately did not address the question of surface mineralogy) as well as recent interpretations of Viking Orbiter multispectral images.

Chapter 4 is a general conclusion and summary of this thesis research and attempts to assess the conclusions gleaned here with respect to data (both current and previous) from other wavelength regions as well as geochemical and mineral stability considerations. This chapter also addresses future directions that this research should take in terms of iron oxide minerals on the martian surface which will hopefully lead to a more complete understanding of the physical, chemical, and mineralogic state of the surface of Mars both currently and during its long evolution.

CHAPTER 2

OBSERVATIONS OF MARS DURING THE 1986 OPPOSITION: 0.7-2.5 μm RELATIVE REFLECTANCE SPECTROSCOPY

ABSTRACT

I have carried out near-infrared (0.7-2.5 μm) spectral observations of Mars during the 1986 opposition at the Mauna Kea Observatory utilizing the University of Hawaii 2.2 m telescope. Spectra were obtained of several martian locations using a continuously variable filter (CVF) spectrometer with a resolution of $\sim$1.25% ($\Delta\lambda/\lambda$). During two separate runs in June and August, I observed approximately 60 distinct spots between 354 ° W and 163 ° W and 32 ° N and 53 ° S at an angular resolution of $\simeq$ 0.5 to 1.5 arcseconds, corresponding to a spatial resolution on Mars of $\simeq$ 200 to 460 km, varying with nightly seeing conditions. These different spots fall roughly into a set of 8 distinct geologic regions: volcanic regions, ridged plains, ridged volcanic plains, scoured plains, impact basins, channels and canyons, densely cratered regions, and layered terrain and ice [after Carr, 1981 and Scott and Tanaka, 1986]. The spectra exhibit typical noise-related or weather-induced errors of less than 4% of the full-scale signal.

In order to analyze these spectral data, spot-to-spot ratios, or relative reflectance spectra, were produced between spectra taken in different geologic regions. Spectral features observed in these ratios can act as indicators of mineralogic differences between areas under consideration.

Perhaps the most striking result obtained from the many ratios taken close

in time and under similar viewing geometries was the consistent lack of noticeable differences between spectra taken of areas which, in geologic maps and Viking Orbiter images, appear to have very different morphologies. This observation leads to several possible conclusions: (a) the spectral feature differences are below the detection limit of these measurements. (b) The spatial resolution of spots observed on Mars was not high enough to merit comparison with medium- to high-resolution Viking Orbiter images and geologic maps (i.e., the local morphology varies significantly within the aperture region and a mixing or averaging effect operates to reduce the spectral feature differences). (c) All of these regions are the same spectrally in the near-IR. It is likely that all three of these effects operate to some degree to prevent spectral features from being observed among the areas measured. Possibility (c) may best explain these results, as it is consistent with several previous studies indicating a mantling of global dust over much of the observed surface. This global dust may not be of uniform composition, but its spectral signature is dominated by contributions from one or two ubiquitous, spectrally active components. The message to Mars orbiting spectroscopy experiments such as the Soviet PHOBOS mission or possibly Mars-94 VIMS is that the spectral differences are small (only a few percent of the continuum) or non-existent among many areas on Mars in the 0.7 to 2.5 μm region on the scale of several hundred kilometers.

INTRODUCTION

Characterization of the surface mineralogy of planetary bodies other than the earth utilizing ground-based observational methods is certainly a major prerequisite for further study of these bodies utilizing earth-orbiting satellites or spacecraft encounter missions. Direct information on the soil and rock mineralogy of a planetary surface can be obtained by studying the spectral reflectance, or the fraction of solar radiation scattered back into space as a function of wavelength, of the surface [e.g., McCord *et al.*, 1978]. In the case of Mars, many of the ground-based telescopic observations in the visible and near-infrared (0.3 to 2.6 μm) have yielded valuable information on ferric oxides, basalts, and hydroxyl mineralogy of the surface [see, for example, McCord and Westphal, 1971; Singer *et al.*, 1979; Sherman *et al.*, 1982; Singer, 1982; and McCord *et al.*, 1982a]. More recent measurements have addressed the possibility of carbonates, nitrates, and sulfates on Mars which have spectral signatures in the near-infrared [Roush *et al.*, 1986; Blaney and McCord, 1988], which is the spectral region of interest in this study. Within this 0.7-2.5 μm region there are absorptions indicative of Fe^{2+} and Fe^{3+} mineralogy, hydroxylated silicates, water and mineral hydrate mixtures, and both telluric and martian H_2O and CO_2 gases and frosts (Table 2.1).

The goals of most observational studies such as this are to produce well calibrated reflectance spectra of specific regions of a planetary surface in order to identify absorption features (and hence composition) for each region. Due to unforseen instrument difficulties and atmospheric conditions, however, such a calibration was not possible. As a result, this chapter presents the results of a study which performed comparisons, or ratios, between spectra obtained of many distinct geologic regions on Mars. Spectral features which show up in ratios between two different regions can act as indicators of compositional differences between them. In theory, this method can also be used to infer the composition of

TABLE 2.1

Major Absorption Bands From 0.7-3.0 μm[†]

Absorber	*Spectral Region* (μm)	*Band Centers* (μm)
H_2O (vapor)	0.70 - 0.74	0.718
	0.79 - 0.84	0.810
	0.926 - 0.978	0.935
	1.095 - 1.165	1.130
	1.319 - 1.498	1.395
	1.762 - 1.977	1.870
	2.520 - 2.845	2.680
H_2O (frost)	1.42 - 1.70	1.56
	1.90 - 2.22	2.04
	2.65 - 3.35	3.00
CO_2 (vapor)	1.38 - 1.50	1.4
	1.53 - 1.67	1.6
	1.92 - 2.11	2.0
	2.63 - 2.87	2.7
CO_2 (frost)	1.41 - 1.47	1.44
	1.57 - 1.62	1.60
	1.86 - 1.88	1.87
	1.96 - 2.13	1.97

TABLE 2.1 (continued)

Major Absorption Bands From 0.7-3.0 μm

Absorber	*Spectral Region* (μm)	*Band Centers* (μm)
CO_2 (frost)	1.96 - 2.13	2.00
	"	2.07
	"	2.12
	2.27 - 2.35	2.28
	"	2.34
	2.61 - 2.78	2.62
	"	2.69
	"	2.77
	2.84 - 2.91	2.85
	"	2.90
	2.99 - 3.02	3.00
Fe^{3+}	0.8 - 1.1	mineral specific
Fe^{2+}	0.9 - 1.25	"
H_2O+ min.hyd.mix.	1.5 - 1.72	"
hydx.silicates (cation—OH)	2.27 - 2.45	"

†gas phases from Blake [1983]; frosts from Kieffer [1970]; others adapted from Hunt *et al.*, [1971, 1973a,b].

an unknown or poorly characterized region which is being compared to one or more well-categorized areas; however, in practice, such inferences are extremely difficult to make. This spot-to-spot comparison method is most useful for high signal-to-noise ratio data acquired on non-photometric nights or for data acquired during times when standard star or standard lunar spot observations were poor or impossible to make due to weather, instrumentation, or viewing geometry problems.

INSTRUMENTATION AND OBSERVATIONS

The spectral studies presented here were performed using the Planetary Geosciences Division (PGD) continuously variable filter (CVF) visible to near-infrared spectrometer with a spectral resolution of ~1.25% ($\Delta\lambda/\lambda$) [see McCord *et al.*, 1978]. Data were obtained over the wavelength range 0.7-2.5 μm. The CVF spectrometer uses an indium antimonide detector which is cooled to solid nitrogen temperature (~77 K). The size of the area to be observed can be controlled by varying the size of the spectrometer entrance aperture. Aperture sizes on this particular instrument range from less than one arc-second to more than ten arc-seconds as projected onto a planetary disc. Once the beam passes through the aperture and the CVF, it is focused onto the detector into an image of the telescope's primary mirror by a small, short focal length Fabry lens. The detector signal is compared to either the signal from a black chopper blade or a nearby dark sky region about once every 150 milliseconds, thus providing a reference zero level. Using an f/35 secondary and the smallest aperture available, spot sizes on the surface of Mars from 200 to 460 km were obtained, depending on nightly seeing conditions.

I carried out the observations of Mars presented in this chapter on the

nights of June 16-23 and July 30-August 4, 1986, universal time, using the University of Hawaii 2.2 m telescope configured with an f/35 Cassegrain focus and chopping secondary. These observations coincided with Mars' best opposition (closest approach) to Earth since 1971; at opposition in mid-July, 1986, Mars was just over 23 arc-seconds in diameter. Figure 2.1 shows just how magnificent the 1986 opposition was: visibility of surface albedo features was excellent, implying also that atmospheric dust opacity was low. This figure, composed of photographs taken through the University of Hawaii's 61 cm telescope atop Mauna Kea, depicts one complete "martian rotation" as seen from Earth during the times of our 2.2 m telescope observations. Since Mars rotates only about 40 minutes slower than the Earth, it takes nearly a month to produce such a series of photographs. From this figure it is obvious that there was no global dust storm activity at or near the 1986 opposition. The areocentric longitude of the Sun (L_s) during the times of observation ranged from 190° to 220°; the martian northern hemisphere was entering the fall season, the southern hemisphere was entering spring. Approximately 60 distinct spots on the surface of Mars located between 354° W and 163° W and 32° N and 53° S were observed (Figure 2.2 and Table 2.2). Additional observations of areas on and near the south polar cap were made during this opposition, but these data will not be discussed here.

DATA ACQUISITION AND REDUCTION

Data were acquired and reduced under the following scheme: first, observations were made at the telescope of each of the individual spots considered. This consisted of careful alignment of the telescope and aperture on a region (using visible albedo features as marker points), and then, through software control, acquisition of raw spectral data through all 120 channels of the

Figure 2.1. 61 cm Planetary Patrol telescope photographs of Mars as seen from Mauna Kea during the times of our 2.2 m telescope observations. Depicted is one "martian rotation" as seen from earth, spanning over a month's time during July and August, 1986. Prominent features include the dark Sinus Meridiani-Sinus Sabaeus region in (a), the bright Tharsis, Amazonis, and Arcadia regions in (d)-(f), the dark Syrtis Major region in (j) and the bright Arabia region in (k). The remnant south polar cap was visible at all times. Red filter photographs. (Courtesy of Lowell Observatory and The National Geographic Society.)

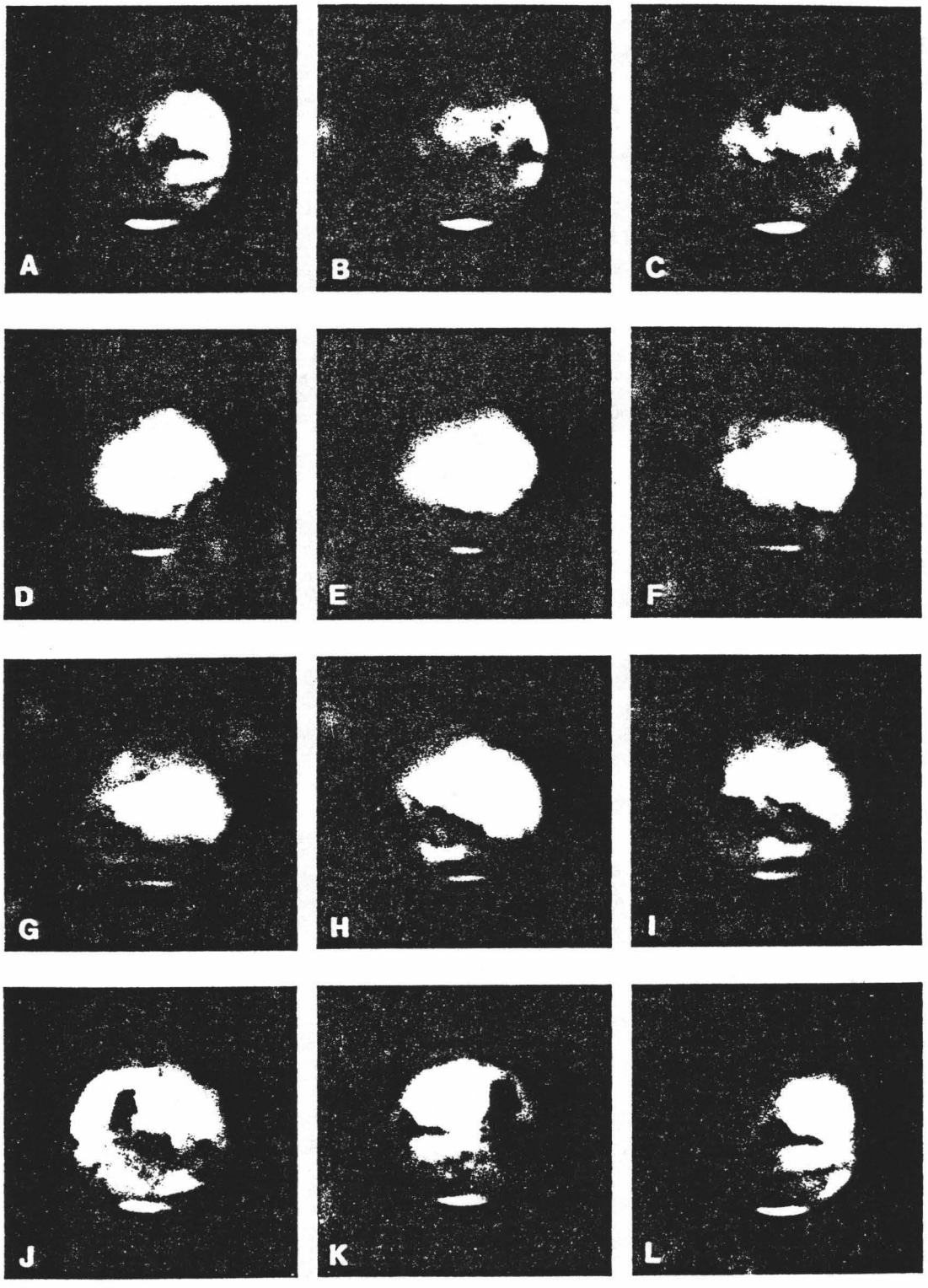
A
B
C
D
E
F
G
H
I
J
K
L

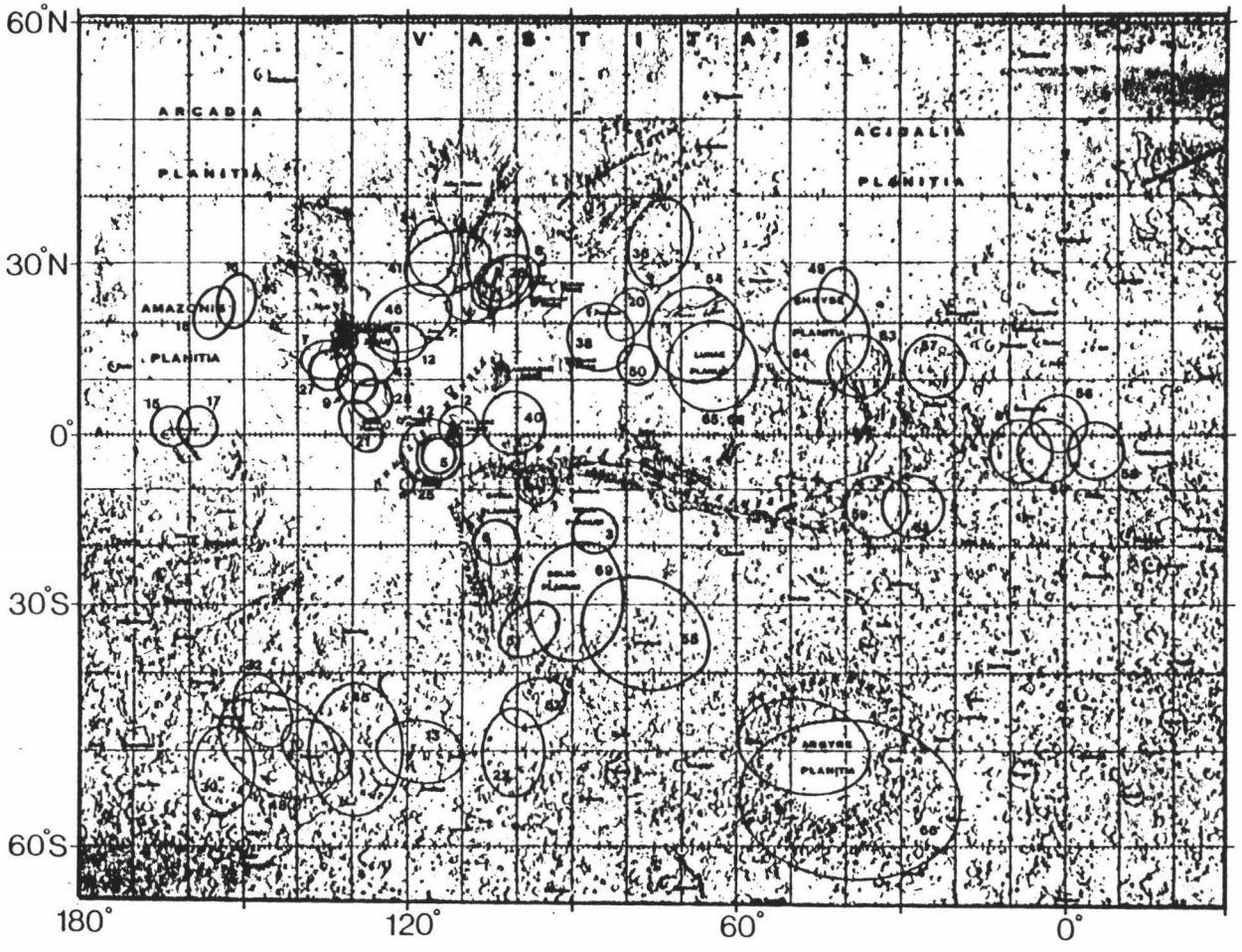

Figure 2.2. Locations on Mars of spots observed for this study during the summer of 1986 (Base map, *U.S. Geological Survey*, Map I-940, 1975).

TABLE 2.2

MARTIAN REGIONS OBSERVED DURING THE 1986 OPPOSITION

Region	Date	Time	Spot #	Lat.	Lon.	LMT[a]	Ap. Size[b]	Runs[c]	Geologic Unit
Alba Patera	6/19	1040	4	+23°	107°	1230	h	3	volcanic
		1159	8	+26	101	1430	h	3	
	6/20	1114	24	+31	115	1200	h	3	
		1221	26	+26	102	1400	h	3	
	6/22	1136	39	+30	103	1200	m	5	
		1233	41	+29	112	1230	m	3	
Amazonis	6/19	1352	15	+1	163	1200	h	3	scoured plains
		1402	16	+23	151	1300	h	3	
		1412	17	+1	158	1230	h	2	
		1418	18	+21	155	1300	h	2	
Argyre Basin	6/22	0957	34	-48	47	1400	m	5	impact basin
	8/04	1000	66	-53	40	1300	l	4	
Chryse	8/01	0808	49	+24	42	1300	h	6	scoured plains
	8/03	1126	54	+17	68	1330	l	3	
	8/04	0702	57	+12	24	1200	m	2	
		0930	64	+17	45	1230	l	5	
Dark Region	6/19	1220	10	-49	136	1230	h	3	dense cratered terrain
		1326	13	-49	117	1430	h	3	
	6/20	1009	22	-49	100	1200	h	3	
		1349	30	-51	153	1200	h	5	
		1419	32	-44	146	1300	h	5	
		1322	45	-48	129	1300	m	5	
		1438	48	-48	143	1330	m	5	
	8/01	1013	52	-43	98	1100	h	5	

TABLE 2.2 (Continued)

MARTIAN REGIONS OBSERVED DURING THE 1986 OPPOSITION

Region	Date	Time	Spot #	Lat.	Lon.	LMT[a]	Ap. Size[b]	Runs[c]	Geologic Unit
Lunae Planum	8/01	0835	50	+12	79	1100	h	5	ridged plains
	8/04	0919	63	+12	38	1230	l	3	
		0947	65	+12	65	1100	l	4	
		1032	68	+12	65	1200	l	5	
Margaritifer	8/04	0746	59	-13	35	1100	m	3	channels/canyons
		0900	62	-13	28	1300	m	5	
Noctus Labyrn.	6/19	0922	1	-9	96	1200	h	3	channels/canyons
Olympus Mons	6/19	1111	7	+13	134	1130	h	2	volcanic
		1209	9	+9	129	1230	h	3	
		1241	12	+16	121	1330	h	3	
	6/20	1231	27	+11	134	1200	h	3	
		1259	28	+6	126	1300	h	3	
	6/22	1253	43	+14	127	1130	m	5	
		1401	46	+20	119	1330	m	5	
Sinai Planum	6/19	1029	3	-17°	85°	1400	h	2	ridged plains
Sinus Meridiani	8/04	0650	56	+2	1	1230	m	4	dense cratered
		0723	58	-3	354	1330	m	6	terrain
		0756	60	-3	3	1330	m	3	
		0839	61	-3	8	1400	m	5	
Solis Planum	8/01	0858	51	-33	99	1000	h	5	ridged plains
	8/03	1142	55	-33	78	1300	l	3	
	8/04	1048	69	-28	90	1030	l	3	

TABLE 2.2 (Continued)

MARTIAN REGIONS OBSERVED DURING THE 1986 OPPOSITION

Region	Date	Time	Spot #	Lat.	Lon.	LMT[a]	Ap. Size[b]	Runs[c]	Geologic Unit
Syria Planum	6/19	1104	6	-19	103	1330	h	2	ridged volc. plains
Tempe Fossae	6/20	0947	20	+21	79	1300	h	3	ridged volc. plains
	6/22	1032	36	+32	73	1300	m	5	
		1119	38	+17	84	1300	m	5	
Tharsis	6/19	1017	2	+1	110	1200	h	2	volcanic
		1051	5	-4	114	1230	h	3	
	6/20	1000	21	+1	128	1000	h	3	
		1124	25	-4	113	1330	h	3	
	6/22	1152	40	+2	100	1330	m	6	
		1244	42	-3	115	1330	m	3	

[a]LMT=Local Martian Time of day that the spot was observed, estimated to the nearest half hour.
[b]Aperture size: h=high res. (≃210 km), m=medium res. (≃330 km), l=low res. (≃460 km)
[c]total number of CVF cycles averaged back-to-back (see text)
All dates and times are UT.

CVF. During the CVF's rotation cycle (all 120 channels take roughly 90 seconds to scan, compare with the chopper blade, display, and write to disc), the telescope and aperture were manually guided on the region observed. A television image obtained from the telescope via a beam splitter was recorded onto videotape during the manual guiding period to record aperture position and guiding accuracy for later analysis. This procedure was repeated from 3 to 5 times back-to-back for each individual spot in order to verify the repeatability of the data, check the manual guiding, and provide a measure of the short-term seeing variations for that night. During a typical evening, the same spot was observed as many as 5 times at up to 2 hour intervals, again, to determine repeatability and accuracy. At frequent periods during the night, the raw data were stored on digital magnetic tape for later processing.

Further data reduction was carried out through the use of an interactive data analysis program specifically designed for use with this type of spectrometer [see Clark, 1980]. The 3 to 5 back-to-back spectra of each spot were averaged and checked for data glitches and signal (guiding) consistency, especially in spectral regions coinciding with telluric water bands. This average thus provides a good representation of signal strength across the 0.7 to 2.5 μm region, as well as an indicator of the typical noise-related or weather-induced error during that particular measurement. Typically, the noise-related or weather-induced error was found to be less than 4% of the full-scale signal. Averaged spectra showing greater errors were usually discarded from this data set, with exceptions occurring for spectra of regions only observed once or twice over the course of both runs. After averaging, ratios, or relative reflectance spectra, were made between several sets of carefully chosen spectra by division of one spectrum by another.

RESULTS AND INTERPRETATIONS

Figure 2.3 summarizes some of the main difficulties involved in interpreting relative reflectance spectra. As emphasized in Figure 2.3.4, it is not realistic to expect to be able to characterize regional mineralogies based on these ratios. This figure does point out, however, that relative reflectance spectra can be very sensitive indicators of subtle differences between areas under consideration. With this distinction in mind, the ratios created were grouped into two somewhat distinct sets: ratios between "similar" and "different" areas. The distinction between "similar" and "different" was made on the basis of both Viking Orbiter mid- to high-resolution images of the regions observed and the geologic map of Scott and Tanaka (1986). Thus, this distinction is based on morphology, lithology, stratigraphy, and structure, and not necessarily composition. Of the many hundreds of ratios possible among the 60 or so spots observed, Figures 2.4 and 2.5 represent those deemed to be the most interesting and informative. As a test of whether compositional differences might be distinguished based on the above distinctions, a "control experiment" was carried out. Areas which, on the Scott and Tanaka (1986) geologic map and in Viking Orbiter images appeared to exhibit similar morphology and/or structure over the spatial extent typical of our Earth-based aperture (for example, the apparently similar volcanic units south of Alba Patera and Southeast of Olympus Mons, or adjacent dark southern hemisphere cratered terrains) were compared. The results (Figure 2.4) do not deviate markedly, on average, from what might be expected: in general, the spectra of regions which appear similar in Orbiter images are nearly the same. There are many sources of error to consider, such as the complications added to the ratios due to the presence of rapidly variable extinction associated with telluric water bands at 0.718, 0.810, 0.935, 1.130, 1.395, and 1.870 μm as well as martian atmospheric and surface (frost) CO_2 bands at

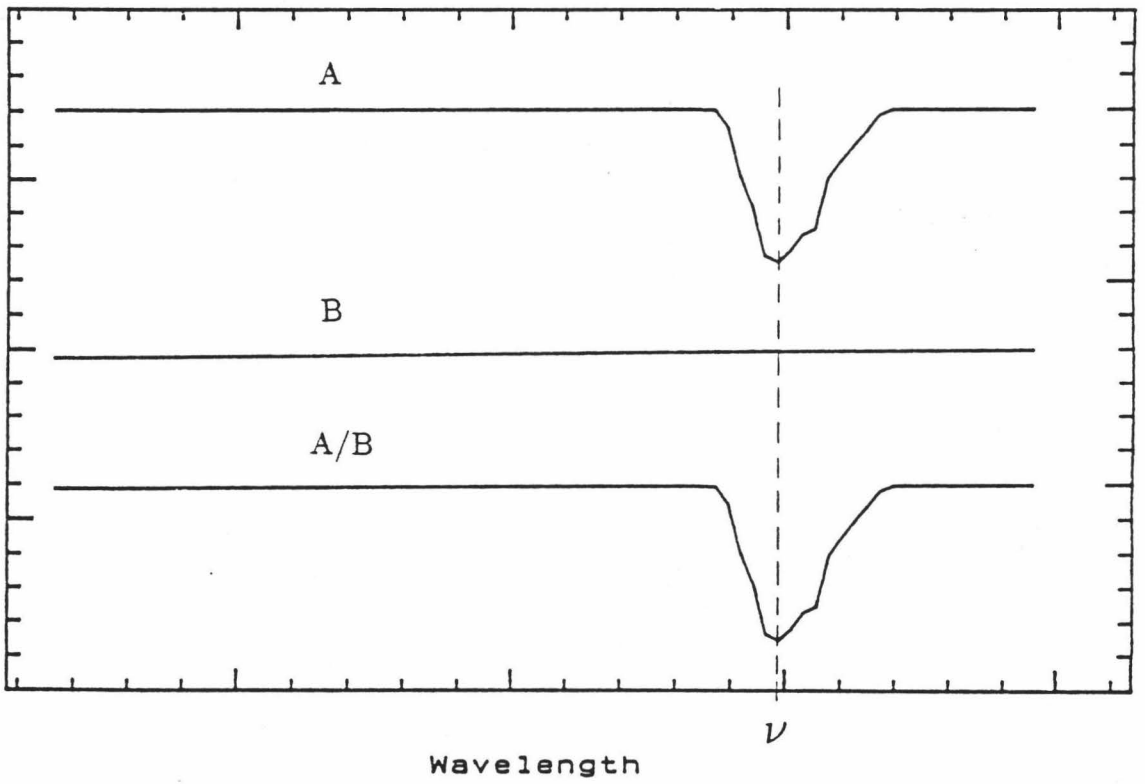

Figure 2.3.1. Simplified analysis of method used in this study to identify observed features appearing in spectral ratios. Feature in spectrum A at wavelength ν but no similar feature at the same wavelength in spectrum B of a different region. The spectral ratio A/B duplicates the feature in A.

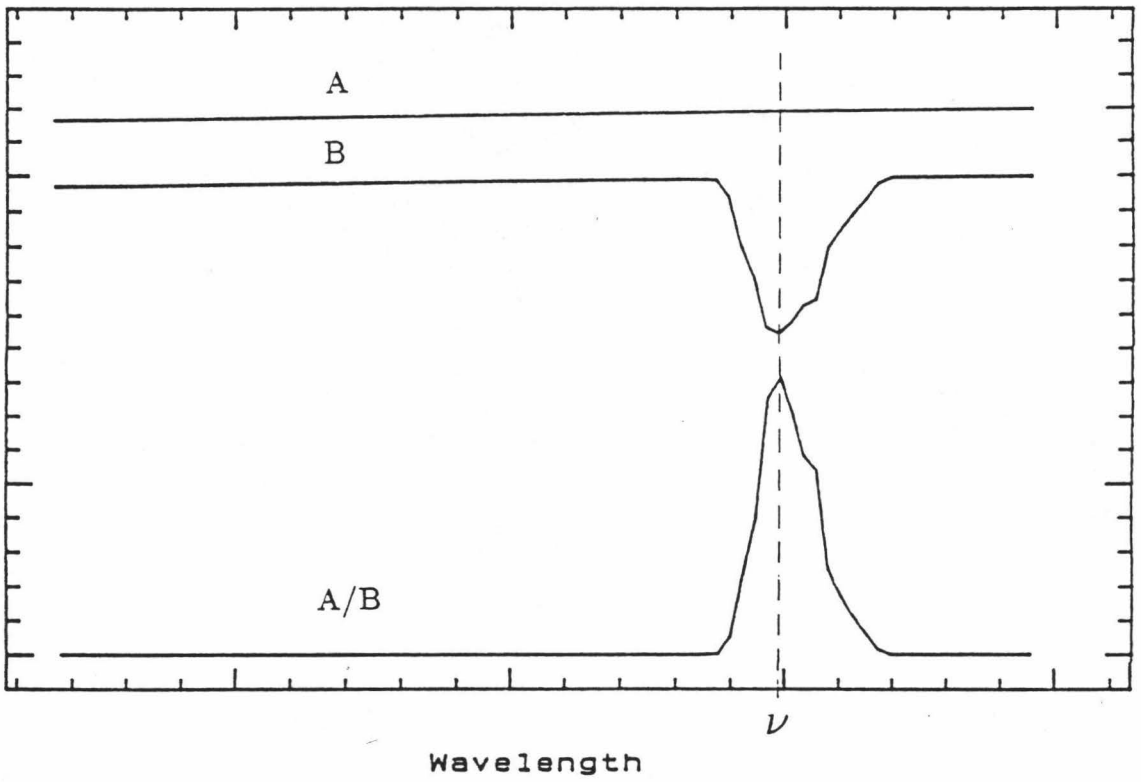

Figure 2.3.2. Similar to Fig. 2.3a but now the feature appears in the spectrum of region B. In this case, the ratio A/B duplicates the feature from B, however it is inverted relative to the surrounding baseline.

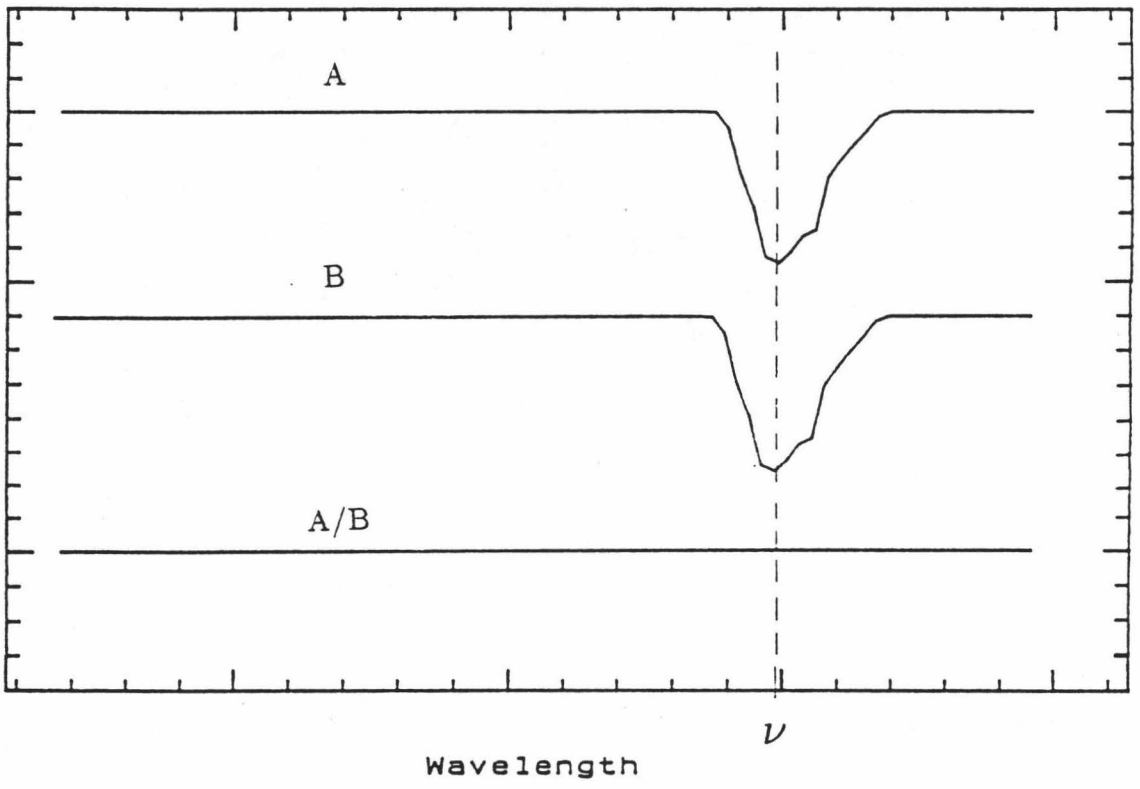

Figure 2.3.3. In this case, both spectra A and B show the same absorption feature at the same wavelength. The ratio A/B is then simply unity.

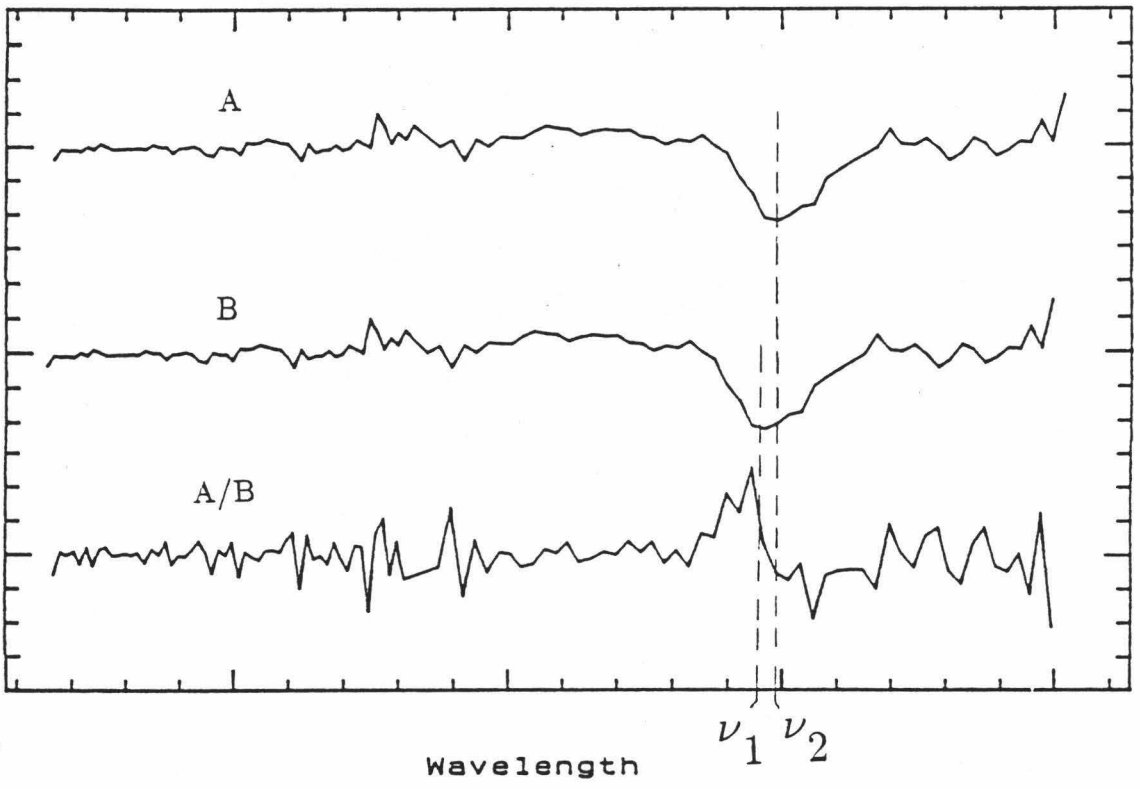

Figure 2.3.4. In this more realistic case, the feature in spectrum A is centered at ν_2 and the feature in spectrum B is centered a small distance apart at ν_1 (as a result of some CVF calibration offset error, for example). In the resulting ratio A/B it is not possible to clearly distinguish features at either ν_1 or ν_2 apart from the surrounding "noise." In fact, the apparently inverted feature just shortward of ν_1 could be erroneously attributed to an absorption from region B which did not appear in region A. Although only an illustrative example, it emphasizes one of the many difficulties with this method.

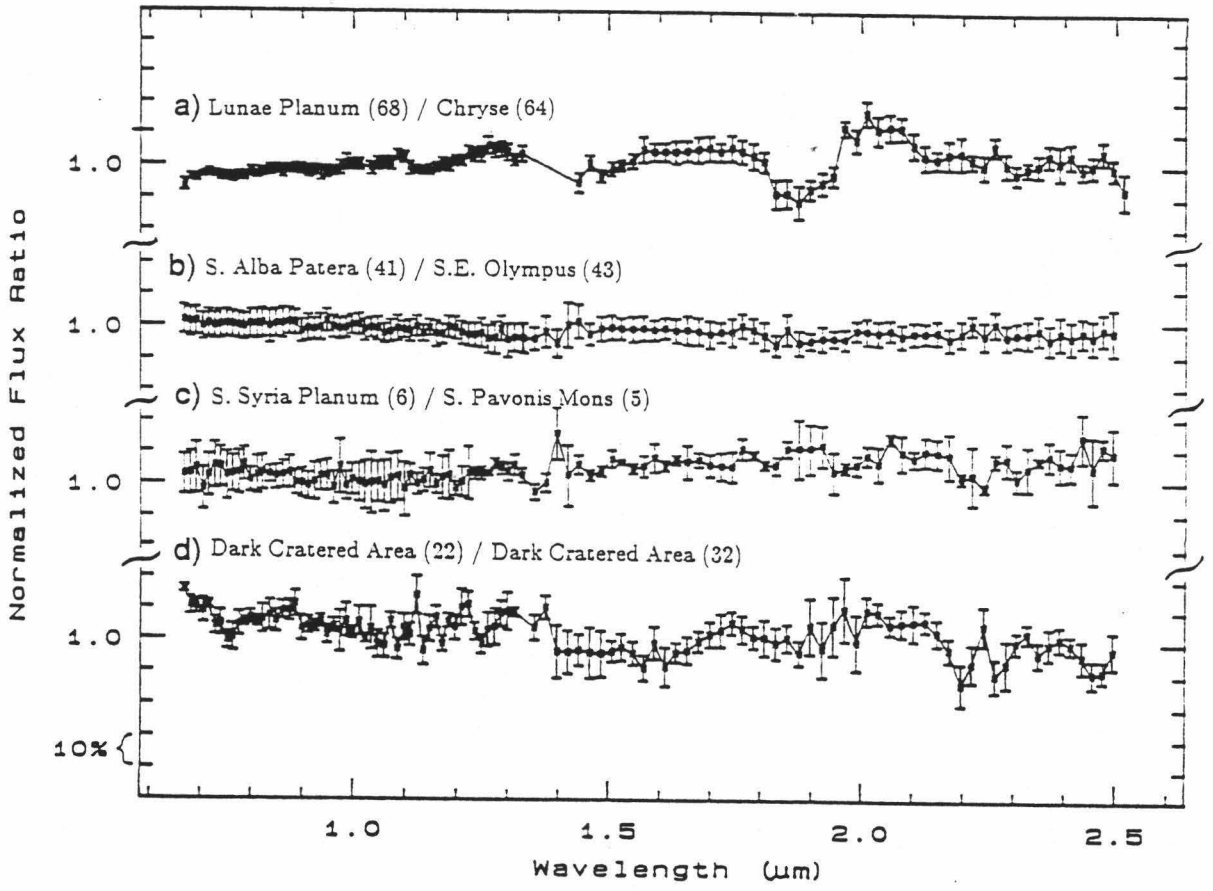

Figure 2.4. Four spectral ratios, or relative reflectance spectra, between "similar" areas based on Viking Orbiter images and geologic mapping [Scott and Tanaka, 1986] of the regions observed. Note the general flatness of these ratios, especially that between the similar volcanic areas to the south of Alba Patera and southeast of Olympus Mons. Most of the features observed in these ratios which deviate outside of 2-3 standard deviations of the noise are associated with telluric water band variations or martian CO_2 variations (Table II-1). (Numbers in parentheses correspond to spot spectra listed in Table II-2.)

1.4, 1.6, and 2.0 μm which all exhibited some degree of time- and space-variable behavior. However, by "same" we mean that the ratios do not exhibit observable, mineralogic features outside of 2-3 standard deviations of the signal. Most features which are seen are associated with the aforementioned telluric water band variations or Mars CO_2 variations.

Figure 2.5 shows the results of ratios created in the second set; those between areas which exhibit different morphology as seen in Viking Orbiter images and the Scott and Tanaka (1986) geologic map. If surface morphology is related to bedrock mineralogy, then the ratios could be expected to show differences among the regions compared due to inferred differences in Fe-bearing minerals, hydroxylated or clay mineral content, H_2O or CO_2 frost cover, etc., expected for clear, observable morphological differences (for example, the Amazonis plains units vs. the summit region of Pavonis Mons, the fossae units south of Alba Patera vs. southern hemisphere dark cratered terrain). However, the spectral ratios are remarkably similar to those observed in Figure 2.4. Except for a few broad slope differences, identifiable features outside at least 2σ of the mean are absent. Again, most observed "features" are associated with telluric H_2O or martian CO_2 variations. In general, distinction by this ratio method of any absorption features which may exist in close proximity to these bands is difficult except under very stable observing conditions, or when spectra are taken close together in time and/or space.

Together, Figures 2.4 and 2.5 show that attempting to distinguish compositional differences based on observable differences in morphology, structure, etc. is not possible for the region of Mars observed and at the spectral and spatial resolutions obtained. The results of this test agree with those of Kieffer *et al.* (1977) who compared Viking albedo and thermal inertia to surface morphology and found little correlation.

Further evidence of this lack of correlation can be seen in Figure 2.6.

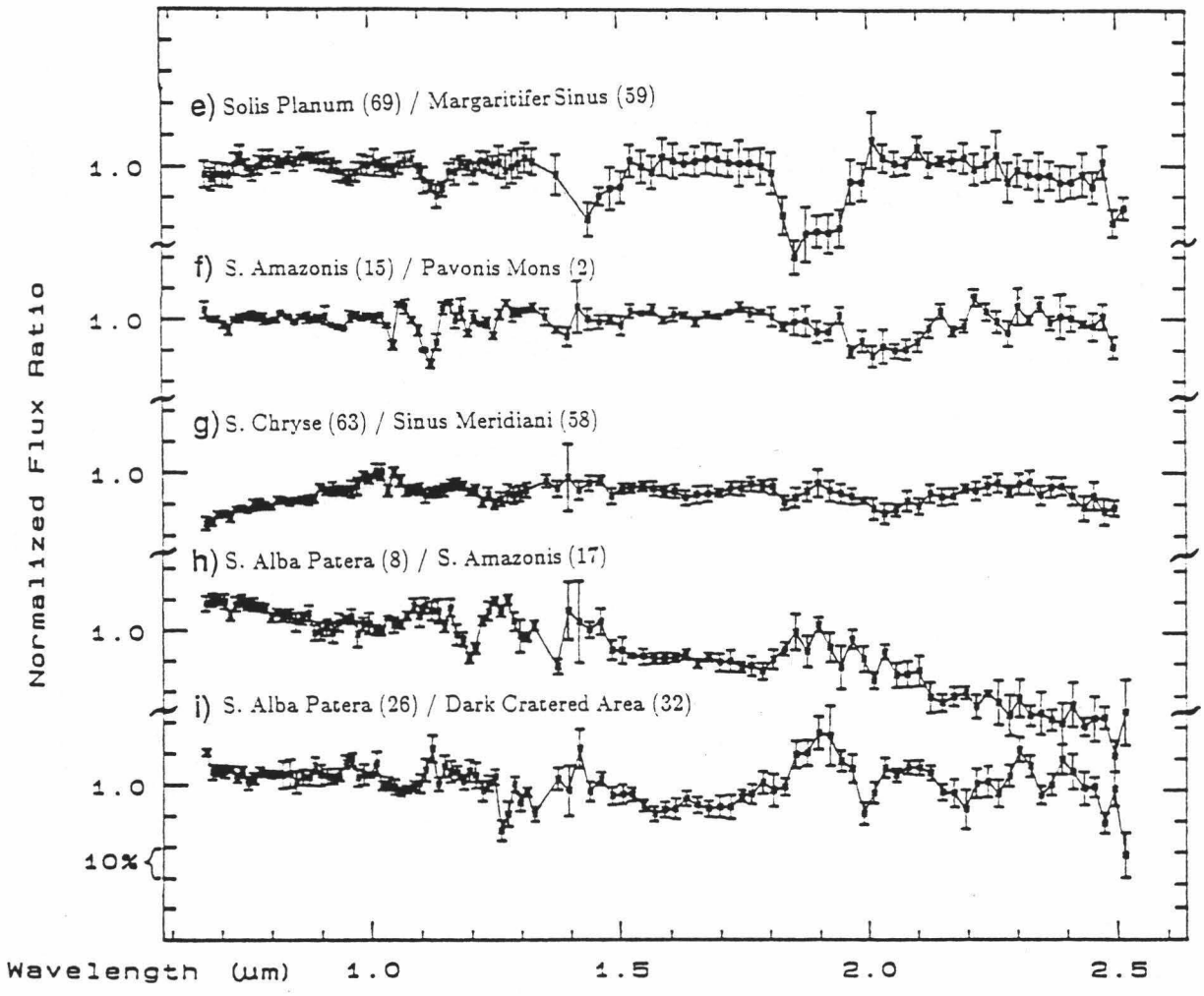

Figure 2.5. Five spectral ratios between "different" areas based on Viking Orbiter images and geologic mapping [Scott and Tanaka, 1986] of the regions observed. The spectra of the regions compared are remarkably similar. As in Figure 2.4, the ratios are generally flat except for a few broad slope differences, most notably the slope drop shortward of 1.0 μm in the ratio between the brighter southern Chryse Planitia region and the darker Sinus Meridiani region. Again, most of the features seen here are associated with telluric H_2O and/or martian CO_2 variations.

This figure depicts the locations of the regions compared in Figures 2.4 and 2.5 with reference to thermal inertia [Palluconi and Kieffer, 1981] and broadband albedo [Pleskot and Miner, 1981] maps of Mars. Ratios a, b, d, e, f, and h from Figures 2.4 and 2.5 are seen to be comparisons between areas of roughly similar thermal inertia and roughly similar albedo, while ratios c, g, and i are between areas which exhibit significant differences in both thermal inertia and albedo. The regions exhibiting similarities among these two surface properties also exhibit similar near-IR reflectance spectra, with the notable exception of ratios d and h, which both show some degree of spectral slope variation (see Chapter III). The converse is not true, however. The regions which exhibit significant differences in thermal inertia and albedo also tend to exhibit similar near-IR reflectance spectra. A possible exception here is ratio i, which compares regions having the greatest differences in thermal inertia and albedo of all the ratios. Ratio i shows a modest degree of slope variation and apparent spectral variation, especially longward of 1.8 μm. Although the spectral differences in this ratio are subtle, they may be indicative of some real chemical or mineralogic difference existing between these two very different areas. Regardless, there appears to be little correlation overall between areas which are similar or different spectrally and those which are similar or different based on a number of other physical and physiographic factors.

Interpretation of these results is certainly not straightforward. Beyond the obvious signal/noise problems and telluric H_2O and martian CO_2 band variations, there are also subtle difficulties with the spectral ratio method itself, as seen previously in Figure 2.3. In the more realistic cases where signal/noise is low or slopes vary differently from spectrum to spectrum, the resulting ratio may not be a sensitive indicator of spectral differences between the two regions.

Additionally, factors such as viewing geometry and solar phase angle can act to produce spectral differences not related to mineralogic variations. Attempts have been made here to minimize these geometric effects by observing Mars at

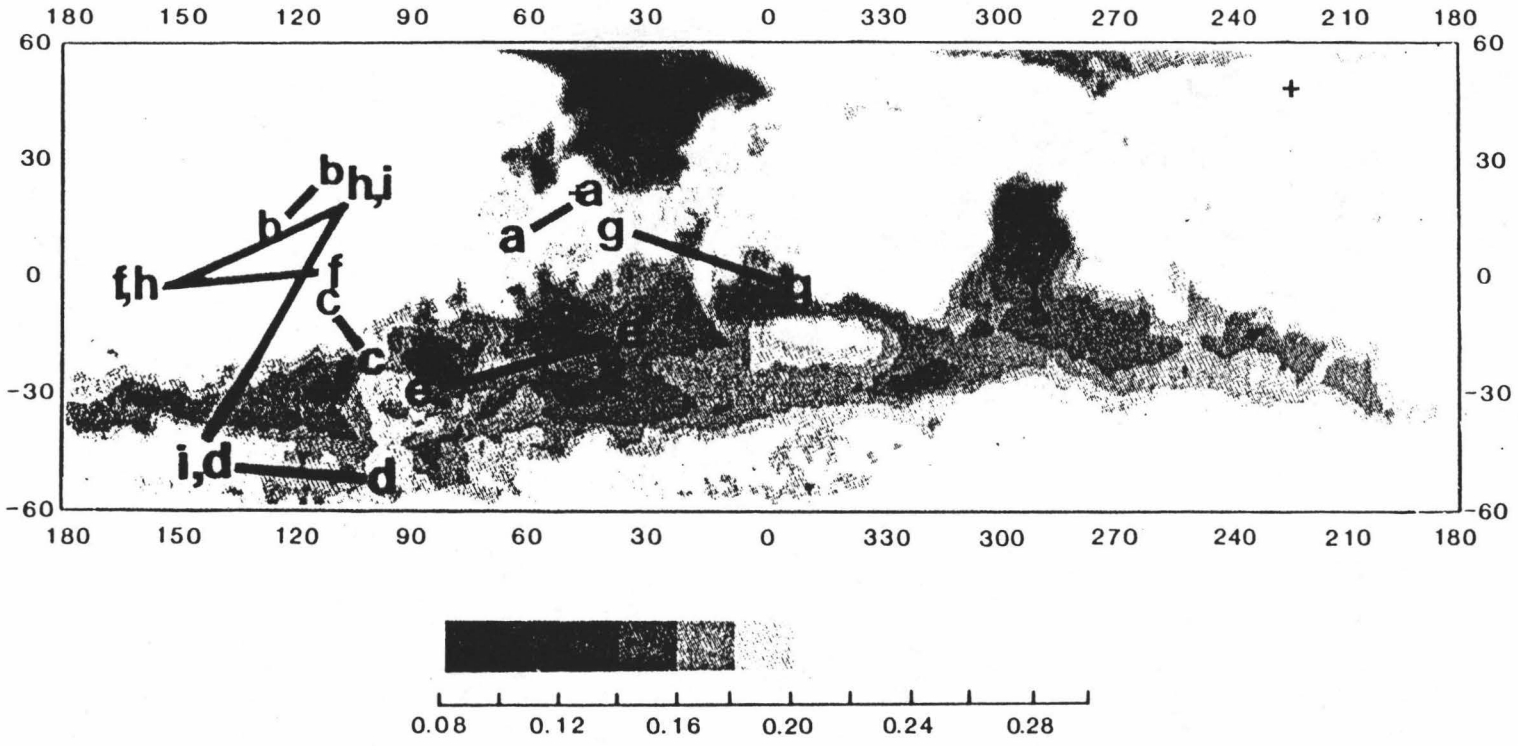

Figure 2.6.1. Locations of regions compared in Figs. 2.4 and 2.5 with reference to Viking Orbiter broadband surface albedo as determined by Pleskot and Miner (1981).

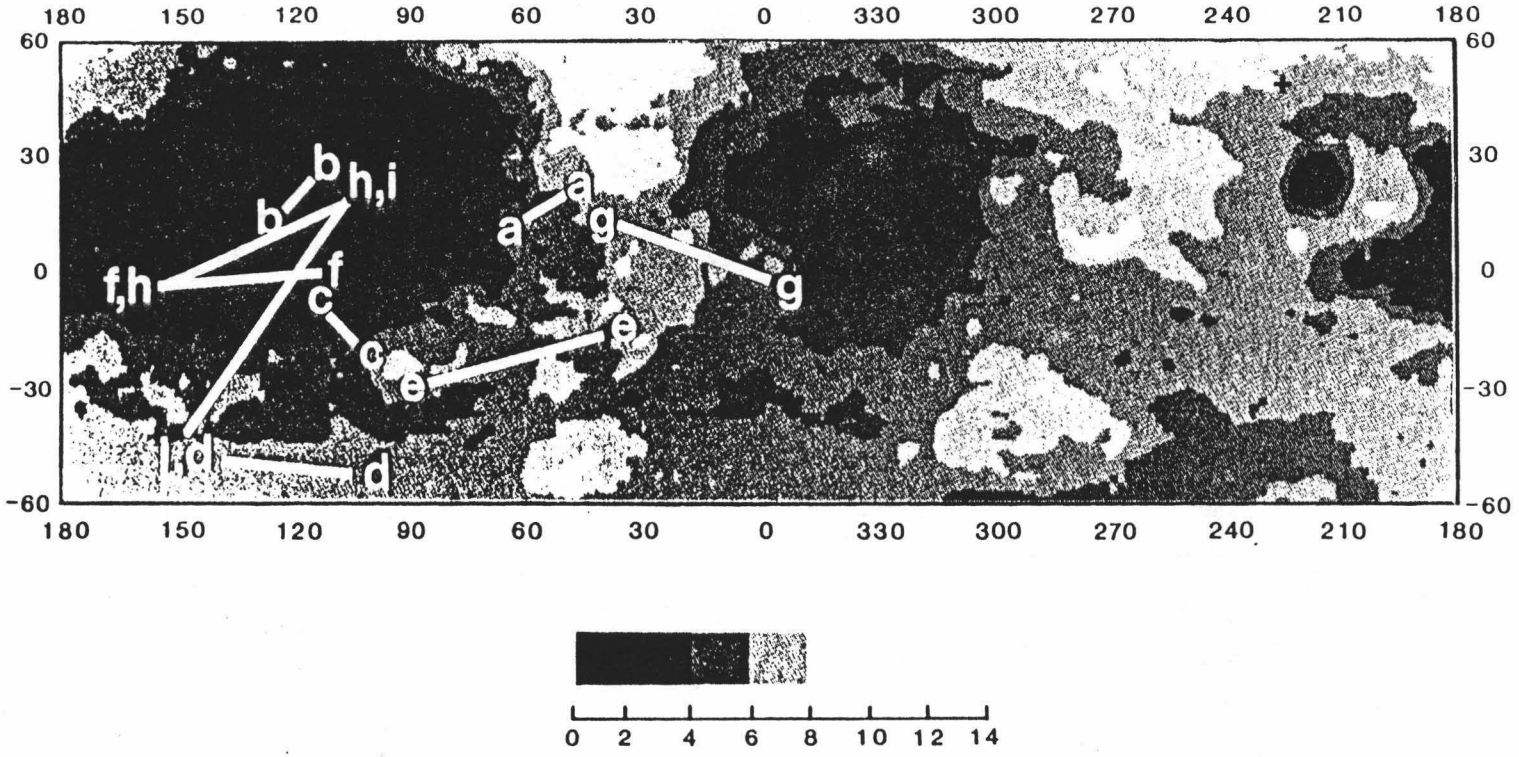

Figure 2.6.2. Locations of regions compared in Figs. 2.4 and 2.5 with reference to Viking Orbiter thermal inertia as determined by Palluconi and Kieffer (1981). Thermal inertia units are 10^{-3}cal cm^{-2}sec$^{-1/2}$ K. Crosses indicate Viking Lander sites.

near-equal intervals around the opposition (nearly equal phase angles) and by observing as many areas as possible as they passed through the center-of-disk, or at least as they passed through the sub-earth central meridian if the regions were not equatorial (Table 2.2). These viewing geometry constraints are yet further added complications which must be considered when attempting to interpret the results. There is hope for the method as applied to these data, however, even in light of the many sources of error. One good sign is that telluric H_2O and martian CO_2 variations did in fact register in the ratios. This provides one measure of the CVF sensitivity/accuracy and attests to the fact that the aperture guiding was fairly accurate (Mars CO_2 variations were seen between high and low regions (e.g. between the high Tharsis shield spectra and the lower plains spectra to the east) and between frost and non-frost surfaces (e.g. between regions just on and off the observable south polar cap), as expected). Yet another good sign was the appearance of slope differences between bright and dark regions, in agreement with previous spectral reflectance results [McCord and Westphal, 1971; McCord *et al.*, 1971; Singer *et al.*, 1979]. The identification of known H_2O and CO_2 features and of expected near-visible slope/albedo differences both lend creedence to the supposition that the otherwise flat spectral ratios observed in Figures 2.4 and 2.5 actually indicate little or no gross spectral (and therefore certain mineralogic) variations between regions observed, at least at the spatial resolution observable from Earth.

CONCLUSIONS AND DISCUSSION

Several possible conclusions can be formulated to explain the lack of prominent spectral differences between areas in this region on Mars:

(a) The measurements were simply not sensitive enough to pick up weak bands or slight differences in band depths between regions. As mentioned before, the identification in the spectra of even some of the weaker telluric H_2O and martian CO_2 bands argues against this conclusion.

(b) The spatial resolution of the spots observed on Mars is inadequate. In other words, the local morphology (and compositional units) varied significantly enough within the aperture that many different compositional units may have "blurred" together producing a common average. Unfortunately, little can be done about this. The 1986 Mars opposition was the best since 1971, and spatial resolution of the telescopic spots was very high (by Earth-based observing standards). The 1988 opposition will be slightly better, affording possible spot resolutions down to $\simeq$180 km under the best viewing conditions.

(c) Or, all the regions observed are spectrally the same in the near-IR.

It is likely that all three of the above effects operate to some degree to prevent distinct spectral features from being observed among the areas measured. There is always hope that improved measurement precision will reveal spectral features, but these measurements, although not the very best, are sufficient that spectral features could be expected. Spatial averaging of different spectral and therefore compositional units within the observed spot size surely occurred to some degree, but the Viking Orbiter images show large-scale morphological differences on the scale of the spot size so that spatially averaging should not completely remove spectral differences if they are associated with morphology. Recent work by Arvidson *et al.* (1987) (reporting Viking Lander spectral evidence for dust deposits in Chryse Planitia and vicinity and suggesting meteorological

control of the outcrop patterns of surficial materials) indicates that materials which contribute to any spatial averaging within the spot size may not all, in fact, be locally derived. This further complicates the process of identification of local bedrock mineralogy, but it reinforces the contention that there are observable spectral differences within the field of view despite spatial averaging.

Possibility (c) may best explain the results of this chapter. First, all or even most morphological units may not be very distinct compositional and spectral units (cf. Kieffer *et al.* 1977). Spectroscopy does not reveal all mineralogies. Differences between various basalts, for example, may be revealed in the spectra only by small differences in absorption bands common to most basalts. Second, there may be very distinct compositional units present on the surface of Mars only as outcrops of small spatial scale within a grossly uniform rocktype or mantle covering a large area, and these could not be revealed in these measurements. Third, a mantling deposit, namely the global dust, may contribute significantly to the spectra of the spots measured here [McCord *et al.*, 1977; Singer *et al.*, 1979; Guinness *et al.*, 1979]. This dust mantling may not be of globally uniform composition; however, data presented here and in Chapter 3 indicate that a single component, spectrally active absorber (hematite) may be ubiquitous across Mars.

These results must be compared with earlier telescopic measurements which are reported to show spectral and mineralogic differences. For example, McCord *et al.* (1971) reported noticeable spectral differences between the bright Arabia region and the darker Syrtis Major region during an extensive observational study of small ($\simeq$200 km diameter) regions on Mars during the 1969 opposition. Singer *et al.* (1979) have reported actual mineralogic differences between several bright and dark areas observed at 1000-2000 km scales during the 1978 opposition. In that study, several absorptions near 1.0 μm in several dark regions were attributed to Fe^{2+}, primarily in pyroxenes. Spectral absorption

evidence was also reported for highly dessicated mineral hydrates and for H_2O-ice and/or adsorbed H_2O. Those spectral and mineralogic differences were reported for areas of Mars which were not observed in this study (compare Figure 2.2 of this chapter with Singer *et al.* 1979, Figure 1). In addition, those differences are generally associated with small amplitude spectral features and some of the data were of higher quality than reported here. Another possibility that must be addressed is that the regions observed on Mars in all studies are not necessarily unchanging with time. For example, McCord *et al.* (1971) reported that Arabia's spectral albedo and brightness changed between March and May 1969. Color and brightness changes were also seen at the Viking Lander sites during the Viking Lander mission [Arvidson *et al.*, 1983; Guinness *et al.*, 1979, 1982]. If martian regions are changing on relatively short timescales (probably as a result of seasonal eolian changes and thus seasonal dust coverage changes), then lack of spectral and mineralogic differences between regions observed may only be, in effect, a transient event. Thus, there is not necessarily a contradiction between earlier measurements and those reported here.

Comparison of the results of this study using Earth-based near-IR spectral data with other conclusions gleaned from Earth-based radar or Viking Orbiter color and Infrared Thermal Mapper (IRTM) data indicates a good degree of correlation. The Viking Orbiter 3-filter global approach mosaic studied by Soderblom *et al.* (1978) and McCord *et al.* (1982b) identified several possible "global dust units" (at >200 km resolutions). The results, however, were not highly conclusive due to brightness and color discrepancies brought on by either phase angle differences between the Orbiter data and groundbased telescopic data, or by actual differences in the degree and distribution of dust coverage between the times the Orbiter observed the surface and the times that groundbased observations were taken. Kieffer *et al.* (1977) report several large, well-defined areas of low thermal inertia where the surface is likely to be covered

by fine material $\leq$ 100 μm in diameter (probably in the range 2-20 μm [Jakosky, 1986]). Typically, the low inertia areas corresponded to the brightest regions observed by the Viking IRTM, which also roughly corresponded to the regions observed during the 1986 opposition. Jakosky and Muhleman (1981) report a good correlation between the 70-cm radar return data of Dyce *et al.* (1967) and the thermal inertia data in this region, although the data are restricted to only one latitude ($\sim$20 $^\circ$ N) and the correlation is not as good at 3.8 or 12.5 cm wavelengths. Overall, other different remote-sensing techniques suggest that much of the observed surface is covered by a fine layer of dust and/or sediments; the 1986 near-IR relative reflectance spectral data support this interpretation.

The message to orbiting spectroscopy experiments planning to study the martian surface, such as the Soviet PHOBOS mission or possibly the Mars-94 VIMS (Visible and Infrared Mapping Spectrometer) investigation, is that the spectral differences are small (only a few percent of the continuum) or non-existent among many areas of Mars on the scale of several hundred kilometers in the visible to near-IR. The large differences that almost surely do exist are probably on a much smaller spatial scale. Further, the Mars global dust, as in the case of the vitrification of the lunar surface material, will reduce the spectral contrast of the surface material and will frustrate (but hopefully not prevent) the detection and interpretation of surface mineralogies. It must be emphasized that the Mars global dust may not be a single composition weathering or alterations product. Instead, it appears most likely that the spectrum of the dust is dominated by one or two fairly ubiquitous, spectrally active components. Serious attention must be paid to orbiting instrument calibration, detection and data system dynamic range, and measurement precision. As well, measurements must be made of as many spots as possible at the highest spatial resolution and with the fullest spectral coverage and resolution.

REFERENCES CITED

Arvidson, R.E., E.A. Guinness, H.J. Moore, J. Tillman, and S.D. Wall, Three Mars years: Viking Lander I imaging observations. *Science, 222*, 463-468, 1983.

Arvidson, R.E., M.A. Dale-Bannister, E.A. Guinness, J. Adams, M. Smith, P.R. Christensen, and R. Singer, Nature and distribution of surficial deposits in Chryse Planitia and vicinity, Mars. Paper presented to the *Workshop on Nature and Composition of Surface Units on Mars,* Lunar and Planetary Institute NASA/MEVTV Study Project, Napa, CA, Dec. 4-5, 1987.

Blake, P.L., Analytical removal of atmospheric absorptions from remotely sensed near-infrared data of geological targets. Unpublished Master's Thesis, University of Hawaii, pp. 25-35, 1983.

Blaney, D.L. and T.B. McCord, Mars: an observational search for carbonates. *J. Geophys. Res.*, in press, 1988.

Carr, M.H., *The Surface of Mars,* 232 pp., Yale Univ. Press, New Haven, 1981.

Clark, R.N., A large scale interactive one dimensional array processing system. *Publ. Astron. Soc. Pac., 92,* 221-224, 1980.

Dyce, R.B., G.H. Pettengill, and A.D. Sanchez, Radar observations of Mars and Jupiter at 70 cm. *Astron. J., 72,* 771-777, 1967.

Guinness, E.A., R.E. Arvidson, D.C. Gehret, and L.K. Bolef, Color changes at the

Viking landing sites over the course of a Mars year. *J. Geophys. Res., 84,* 8355-8364, 1979.

Guinness, E.A., C.E. Leff, and R.E. Arvidson, Two Mars years of surface changes seen at the Viking landing sites. *J. Geophys. Res.,87,* 10,051-10,058, 1982.

Hunt, G.R., L.M. Logan and J.W. Salisbury, Mars: components of infrared spectra and the composition of the dust cloud. *Icarus, 18,* 459-469, 1973a.

Hunt, G.R., J.W. Salisbury, and C.J. Lenhoff, Visible and near-infrared spectra of minerals and rocks: III. oxides and hydroxides. *Modern Geology, 2,* 195-205, 1971.

Hunt, G.R., J.W. Salisbury, and C.J. Lenhoff, Visible and near-infrared spectra of minerals and rocks: VI. additional silicates. *Modern Geology, 4,* 85-106, 1973b.

Jakosky, B.M., On the thermal properties of martian fines. *Icarus, 66,* 117-124, 1986.

Jakosky, B.M. and D.O. Muhleman, A comparison of the thermal and radar characteristics of Mars. *Icarus, 45,* 25-38, 1981.

Kieffer, H., Spectral reflectance of CO_2-H_2O frosts. *J. Geophys. Res., 75,* 501-509, 1970.

Kieffer, H.H., T.Z. Martin, A.R. Peterfreund, B.M. Jakosky, E.D. Miner, and F.D. Palluconi, Thermal and albedo mapping of Mars during the Viking primary

mission. *J. Geophys. Res., 82,* 4249-4292, 1977.

McCord, T.B., R.L. Huguenin, D. Mink, and C. Pieters, Spectral reflectance of martian areas during the 1973 opposition: photoelectric filter photometry 0.33-1.10 μm. *Icarus, 31,* 25-39, 1977.

McCord, T.B., R.B. Singer, B.R. Hawke, J.B. Adams, D.L. Evans, J.W. Head, P.J. Mouginis-Mark, C.M. Pieters, R.L. Huguenin, and S.H. Zisk, Mars: definition and characterization of global surface units with emphasis on composition. *J. Geophys. Res., 87,* 10,129-10,148, 1982b.

McCord, T.B. and J.A. Westphal, Mars: narrow-band photometry, from 0.3 to 2.5 microns, of surface regions during the 1969 apparition. *Astron. J., 168,* 141-153, 1971.

McCord, T.B., J.H. Elias, and J.A. Westphal, Mars: the spectral albedo (0.3-2.5μ) of small bright and dark regions. *Icarus, 14,* 245-251, 1971.

McCord, T.B., R.N. Clark, and R.L. Huguenin, Mars: near-infrared spectral reflectance and compositional implication. *J. Geophys. Res., 83,* 5433-5441, 1978.

McCord, T.B., R.N. Clark, and R.B. Singer, Mars: near-infrared spectral reflectance of surface regions and compositional implications. *J. Geophys. Res., 87,* 3021-3032, 1982a.

Palluconi, F.D., and H.H. Kieffer, Thermal inertia mapping of Mars from 60 ° S to 60 ° N. *Icarus, 45,* 415-426, 1981.

Pleskot, L.K., and E.D. Miner, Bolometric albedo variations of bright and dark regions during the Viking mission. In *Third International Colloq. Mars,* pp. 208-210. Lunar Planet. Inst., Houston, 1981.

Roush, T.L., D. Blaney, T.B. McCord, R.B. Singer, Carbonates on Mars: searching the Mariner 6 and 7 IRS measurements (abstract). *Lunar and Planetary Science XVII,* 732-733, Lunar and Planetary Institute, Houston, Texas, 1986.

Scott, D.H. and K.L. Tanaka, Geologic map of the western equatorial region of Mars. *U.S. Geological Survey,* 1:15,000,000 geologic map, Map I-1802-A, 1986.

Sherman, D.M., R.G. Burns, and V.M. Burns, Spectral characteristics of the iron oxides with application to the martian bright region mineralogy. *J. Geophys. Res., 87,* 10,169-10,180, 1982.

Singer, R.B., Spectral evidence for the mineralogy of high-albedo soils and dust on Mars. *J. Geophys. Res., 87,* 10,159-10,168, 1982.

Singer, R.B., T.B. McCord, R.N. Clark, J.B. Adams, and R.L. Huguenin, Mars surface composition from reflectance spectroscopy: a summary. *J. Geophys. Res., 84,* 8415-8426, 1979.

Soderblom, L.A., K. Edward, E.M. Eliason, E.M. Sanchez, and M.P. Charette, Global color variations on the martian surface. *Icarus, 34,* 444-464, 1978.

CHAPTER 3

OBSERVATIONS OF MARS DURING THE 1988 OPPOSITION: 0.4-1.0 μm SPECTRAL REFLECTANCE AND RELATIVE REFLECTANCE SPECTROSCOPY

ABSTRACT

I have carried out visible to near-IR (0.4-1.0 μm) spectral observations of Mars during the 1988 opposition at Mauna Kea Observatory using a circular variable filter spectrometer at a spectral resolution $R = \lambda/\Delta\lambda \simeq 80$. On August 13 and 14 UT 1988, just 6 weeks prior to opposition, 41 regions 500-600 km in diameter predominantly in the western hemisphere at latitudes $< 30^\circ$ N were observed on Mars. The data have been reduced to reflectance relative to solar analog (Mars/16 Cyg B) and to relative reflectance spectra. The spectra show the strong near-UV reflectance dropoff characteristic of Mars. Of more interest are absorptions at 0.62-0.72 μm and 0.81-0.94 μm seen here clearly for the first time. These features are interpreted as Fe^{3+} electronic transition features that indicate the presence of *crystalline* ferric oxide or hydroxide minerals on the martian surface. Comparison of these data with laboratory data obtained by other workers supports previous conclusions that a single iron oxide phase, most likely hematite, *could* account for all of the observed spectral behavior of the martian surface soils and airborne dust in the 0.4-1.0 μm region. If correct, this conclusion must be reconciled with data from other wavelength regions as well as geochemical and mineral stability considerations to arrive at a more complete understanding of this particular aspect of martian surface mineralogy.

INTRODUCTION

Spectroscopic observations of the planet Mars in the visible to near-IR wavelength range (0.4-1.0 μm) have been ongoing in earnest for nearly a century. The orbits of Earth and Mars bring the two planets to opposition every 25 months, however due to the eccentricity of the martian orbit, the angular size of Mars from Earth at opposition varies from 8 arcseconds when opposition coincides with martian aphelion, to 25 arcseconds when martian perihelion and opposition occur in the same year. Such perihelic oppositions occur every 15-17 years and only during those events are relatively high spatial resolution measurements ($\geq$ few hundred km) able to be made. The most favorable oppositions clustered around perihelion usually occur in groups of three: the previous group occurred in 1969-1971-1973, with the 1971 opposition being the best. Within the current 1986-1988-1990 group, the 1988 opposition is the best, with Mars having reached an apparent angular diameter of nearly 25 arcseconds. Since there was little dust storm activity during the times of observation, the atmosphere was free of optically thick airborne dust and spectral reflectance measurements of mostly surficial materials were made.

Earlier measurements have clearly showed the spectral reflectance curve of Mars to be quite distinctive [*i.e.* de Vaucouleurs, 1964; Younkin, 1966; Tull, 1966; see McCord and Adams, 1969 for a summary]. Most notable is the sharp dropoff in reflectance shortward of 0.7 μm, giving Mars its distinctive red coloration. A flurry of activity associated with the 1969-1971-1973 oppositions, using newer spectroscopic techniques, built on the inferences of these early studies using higher precision ($R = \lambda/\Delta\lambda \simeq$ 18-20) reflectance curves. For example, the work of McCord and Westphal (1971) and McCord *et al.* (1971, 1977) concentrated on quantifying the differences in reflectance properties of bright and dark materials and led to the basic conclusion that bright and dark regions on the planet most

likely corresponded to different mineralogic units. Later work (see for example Hunt *et al.*, 1973a; McCord *et al.*, 1978, 1982; Singer *et al.*, 1979; Singer, 1982; Banin *et al.*, 1985) has concentrated on the identification of these mineralogic units using higher precision measurements both of Mars and of numerous terrestrial samples which appear to be Mars surface soil analogs.

Laboratory spectroscopic studies have shown that electronic transitions and charge transfers by d-shell electrons in ferric iron are primarily responsible for the overall shape of the martian spectral curve in the visible to near-IR (Adams, 1968; Morris and Neely, 1981; Sherman *et al.*, 1982; Sherman and Waite, 1985; Morris *et al.*, 1985). Various workers have postulated on the potential iron-bearing phases which exist on Mars. Dollfus (1957), Sharanov (1961), Hovis (1965), Sagan *et al.* (1965), and Pollack and Sagan (1967) argued for the existence of goethite (αFeOOH) or limonite ($Fe_2O_3 \cdot nH_2O$) on the martian surface based on polarization data and on the shape of the visible to near-IR spectral curve. Later work based on Viking Lander XRF spectrometer data (Toulmin *et al.*, 1977) found the total iron content of the martian soils to be ~18 wt%. Although no direct mineralogic information was obtained from the Viking mission, Toulmin *et al.* (1977) suggested that nontronite (an Fe^{3+}-bearing smectite clay) may account for much of the iron mineralogy. Additionally, a certain component of the iron was found to be highly magnetic and was interpreted by Hargraves *et al.* (1977) to be due to fine-grained maghemite (γFe_2O_3) dispersed throughout the surface soils in quantities of up to 1-7 wt%. Due to the lack of high spectral resolution spacecraft instrumentation, telescopic reflectance spectroscopy continues to provide the most valuable information with which to constrain the surface mineralogy of Mars. More recent interpretations of spectra obtained in the early to late 1970's have suggested that palagonite, the X-ray amorphous weathering product of mafic volcanic glass, may be the best spectral analog to the Mars soils (Toulmin *et al.*, 1977; Soderblom and Wenner, 1978; Gooding and Keil, 1978;

Singer, 1982). A geochemically stable material under current Mars conditions, certain palagonites show the sharp, smooth near-UV absorption edge characteristic of many Mars spectra. The lack of specific, well-defined crystalline Fe^{3+} absorption bands in the spectral data suggested that amorphous, glassy soils must be abundant on the surface, rather than crystalline ferric oxides, hydroxides, or iron-bearing clays.

This chapter details a series of new spectral observations of Mars obtained during the extremely favorable 1988 opposition in the 0.4-1.0 μm wavelength range. These new data, acquired at moderate spectral resolution ($R \simeq 80$) are of higher precision and higher spectral sampling interval than any previously published studies of the martian surface in this spectral region. The goals of this part of the thesis research are to (a) present new spectral reflectance and relative reflectance data for a number of distinct spots on the martian surface at 500-600 km spatial resolution, (b) to compare these data with previous measurements, and (c) to interpret these data in terms of potential surface soil and airborne dust iron mineralogies, with particular interest in the degree of crystallinity of the surface materials.

INSTRUMENTATION AND OBSERVATIONS

I carried out the spectral studies presented here using the Planetary Geosciences Division (PGD) circular variable filter (CVF) spectrometer which covers the 0.4-1.0 μm wavelength region. The CVF spectrometer uses a silicon photodiode detector which is cooled to liquid nitrogen temperature to reduce instrument noise. The filter itself is divided into two sections which cover 0.37-0.713 μm and 0.679-1.094 μm. The spectrometer as configured for these observations had 4 different aperture sizes available, ranging from 1.75 to 13.6

arcseconds as projected onto a planetary disk. Light from a small, selected region of the planet passes through the aperture and the CVF and is focused onto the Si photodiode by a series of camera optics. The detector signal is then compared to the signal from a nearby dark sky region (chopping offset was nearly 1 arcminute) every 150 msec, providing a sky background level which is subtracted from the Mars signal. The aperture position on the planet is carefully monitored and recorded on videotape during the observations. Later analysis of the tape allows accurate determination of spot sizes and positions.

Observations of Mars discussed here were carried out on the nights of August 13 and 14, 1988, universal time, using the University of Hawaii/Air Force 61-cm telescope configured with an $f/35$ chopping secondary. In this configuration, using the smallest aperture available, spot sizes on the surface of Mars from 500-600 km were obtained, depending on nightly seeing conditions. The observations were made at a phase angle of 34° (91% illumination) just six weeks prior to opposition and at a areocentric longitude (L_s) of 250° (late southern spring). The planet was just under 19 arcseconds in diameter. As can be seen in Figure 3.1, there was no planetwide dust storm during most of this opposition. In general, surface albedo markings were distinct throughout most of the summer and early fall (a global dust storm did apparently develop in late November, however [Eicher and Troiani, 1989]). Measurements were made of 41 distinct spots on the surface of Mars located between longitudes 0° W and 200° W and latitudes 70° S and 30° N (Figure 3.2 and Table 3.1). Due to the geometry of this opposition, the subearth latitude was located at 20° S, so much of the northern hemisphere was not observable. Additionally, some measurements were made on and near the still prominent south polar cap; however these data will not be discussed here.

Figure 3.1. Mars as seen from Mauna Kea Observatory during the times of our 61 cm telescope observations. Shown is one complete martian revolution. The 1988 opposition afforded exceptional opportunities to view Mars, and as is evident from these photographs, the pre-opposition global dust storm which many observers feared never came to pass. Spectra of small regions on Mars reported in this paper were obtained predominantly from the western hemisphere of the planet, corresponding to the first five photographs in the sequence.

1988 MARS from MAUNA KEA OBSERVATORY

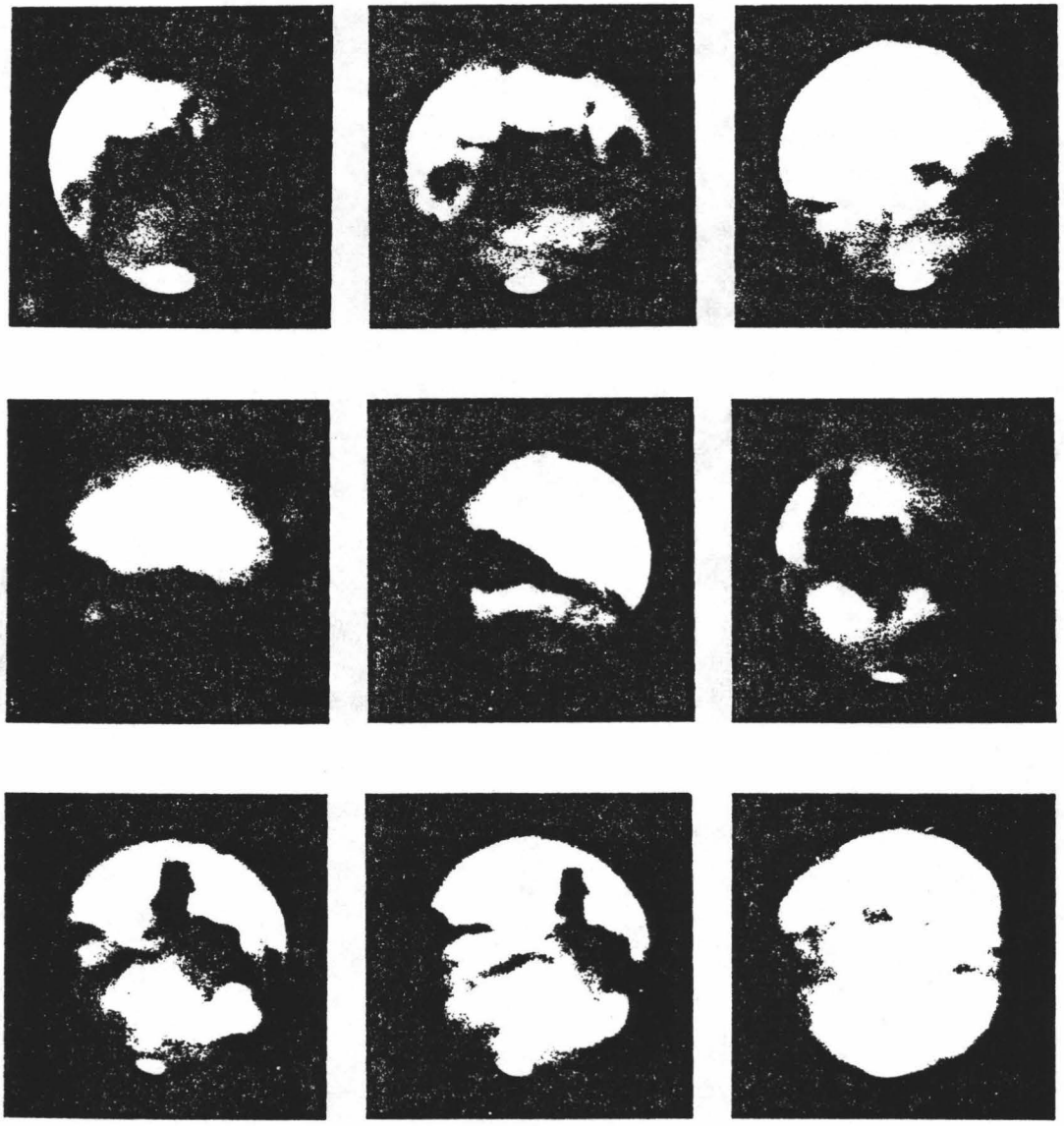

TELESCOPIC MONITORING MARS

Sponsored by THE NATIONAL GEOGRAPHICAL SOCIETY

LOWELL OBSERVATORY/THE UNIV. OF MISSOURI, ST. LOUIS

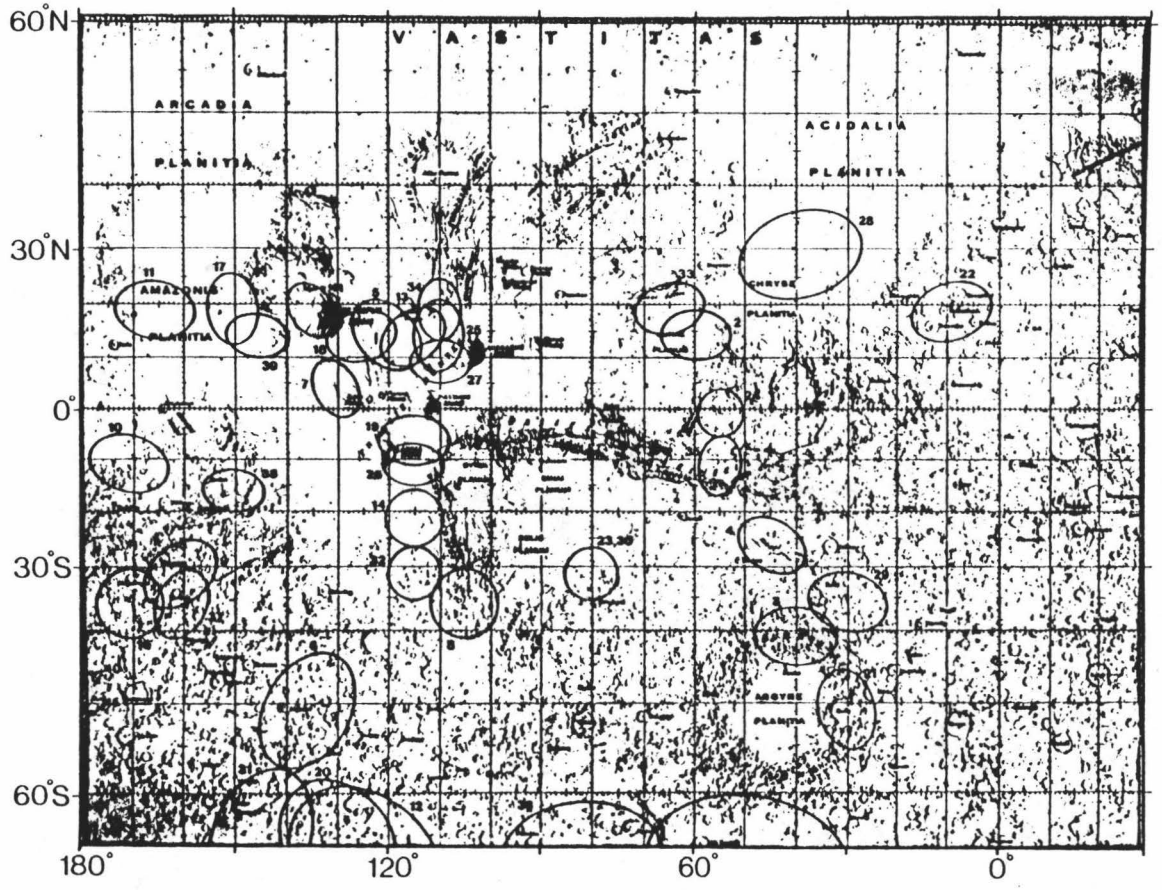

Figure 3.2. Locations on Mars of spots observed for this study during the 1988 opposition. See also Table III-1 (base map U.S. Geological Survey shaded relief map I-940, 1975).

TABLE 3.1

MARTIAN REGIONS OBSERVED DURING THE 1988 OPPOSITION

Region	*Date (UT)*	*Time (UT)*	*LMT*[a]	*Spot no.*	*Lat.*	*Lon.*	*Radius (km)*	*Runs*[b]	*Albedo*[c]	*Geologic Unit*[d]
Amazonis	8/13	1353	1000	11	+20°	165°	300	3	b	Ridged Plains
		1505	1230	17	+20	150	300	2	b	
	8/14	1338	1100	39	+15	145	250	3	b	
Argyre	8/13	1030	1500	1	-65	50	300	6	i	Etched Hilly Terrain
		1051	1600	3	-40	40	300	4	i	
	8/14	0926	1430	21	-50	30	250	4	i	
		1139	1630	29	-35	30	250	3	i	
Aurorae	8/13	1058	1530	4	-25	45	300	3	d	Hilly Cratered Terrain
	8/14	1307	1630	35	-10	55	250	3	d	
Australe	8/13	1133	1000	6	-50	135	300	3	i	Densely Cratered Terrain
		1358	1300	12	-65	125	300	4	i	
		1515	1400	20	-65	130	300	2	i	
	8/14	1156	0900	31	-65	145	250	3	i	
		1315	1430	36	-65	80	250	3	i	
Chryse	8/14	1019	1330	24	+0	55	250	3	i	Ridged Plains
Claritas	8/13	1332	1400	8	-35	105	300	4	i	Densely Cratered Terrain
	8/14	1205	1130	32	-30	115	250	3	d	
Electris	8/13	1457	0900	15	-50	200	300	2	d	Ridged Cratered Terrain
	8/14	1345	0800	40	-45	190	250	3	d	
Lunae Planum	8/14	1213	1430	33	+20	65	250	3	i	Ridged Plains
Memnonia	8/14	1331	1030	38	-15	150	250	3	i	Densely Cratered Uplands

TABLE 3.1 (Continued)

MARTIAN REGIONS OBSERVED DURING THE 1988 OPPOSITION

Region	*Date (UT)*	*Time (UT)*	*LMT*[a]	*Spot no.*	*Lat.*	*Lon.*	*Radius (km)*	*Runs*[b]	*Albedo*[c]	*Geologic Unit*[d]
Mesogaea	8/13	1348	1000	10	-10	170	300	3	i	Densely Cratered Terrain
Olympus Mons	8/13	1127	1100	5	+15	120	300	3	b	Volcanic Plains
		1322	1200	7	+5	130	300	3	b	
		1404	1400	13	+15	115	300	3	b	
		1508	1430	18	+15	125	300	2	b	
		1353	1130	41	+20	135	250	2	b	
Oxia	8/14	0948	1600	22	+20	10	250	4	i	Ridged Plains
Sirenum	8/13	1342	1030	9	-30	160	300	3	d	Densely Cratered Terrain
		1501	1100	16	-35	170	300	2	d	
	8/14	1323	0930	37	-35	160	250	3	d	
Solis Lacus	8/14	1002	1130	23	-30	80	250	3	i	Densely Cratered Terrain
		1147	1300	30	-30	80	250	3	i	
Tharsis	8/13	1410	1400	14	-20	115	300	2	i	Volcanic Plains
		1512	1500	19	-5	115	300	2	b	
	8/14	1102	1030	25	+15	110	250	3	b	
		1110	1030	26	-10	115	250	3	b	
		1119	1100	27	+10	110	250	2	b	
		1259	1230	34	+20	110	250	3	b	
Xanthe	8/13	1045	1400	2	+15	60	300	4	i	Ridged Volcanic Plains
	8/14	1131	1530	28	+30	40	250	3	i	

[a]LMT=Local Martian Time of day that the spot was observed, estimated to the nearest half hour.
[b]total number of CVF cycles averaged back-to-back (see text)
[c]Telescopic visual "albedo": d=dark (≤0.12), i=intermediate (0.12-0.18), b=bright (≥0.18)
[d]roughly based on geologic maps of Scott and Tanaka (1986) and Greeley and Guest (1987)

DATA ACQUISITION AND REDUCTION

The method whereby the raw spectral data were obtained at the telescope is nearly identical to the method outlined in Chapter 2 (Bell and McCord [1989]) for a similar observational study at longer wavelengths during the 1986 opposition. Data reduction in Chapter 2 was hampered by difficult weather conditions which did not allow the acquisition of standard star data. A similar problem was encountered on the first night of these observations (August 13, 1988 UT), and reduction of those data has concentrated on the production of relative reflectance spectra (raw spectral flux ratios), similar to those produced using the 1986 data of Chapter 2. The second night of observations (August 14, 1988 UT) was photometric, however, and standard star observations were performed using the G8III stars αAqr and ηPsc (Figure 3.3). Multiplying the Mars/αAqr data by a previously obtained αAqr/16 Cyg B ratio (16 Cyg B is a G5V class star which is generally regarded as an excellent solar analog) allowed production of approximate reflectance spectra (~Mars/Sun). Nearly all the data reduction was performed with a one-dimensional array processing system specifically designed for use with PGD spectrometers (Clark, 1980). Typically, the variation in signal was found to be less than 3-5% over the course of several CVF rotation cycles. When larger variations were encountered during data reduction, they were usually associated with telluric atmospheric water band variations (light cirrus or transient moist air pockets) or telescopic guiding errors.

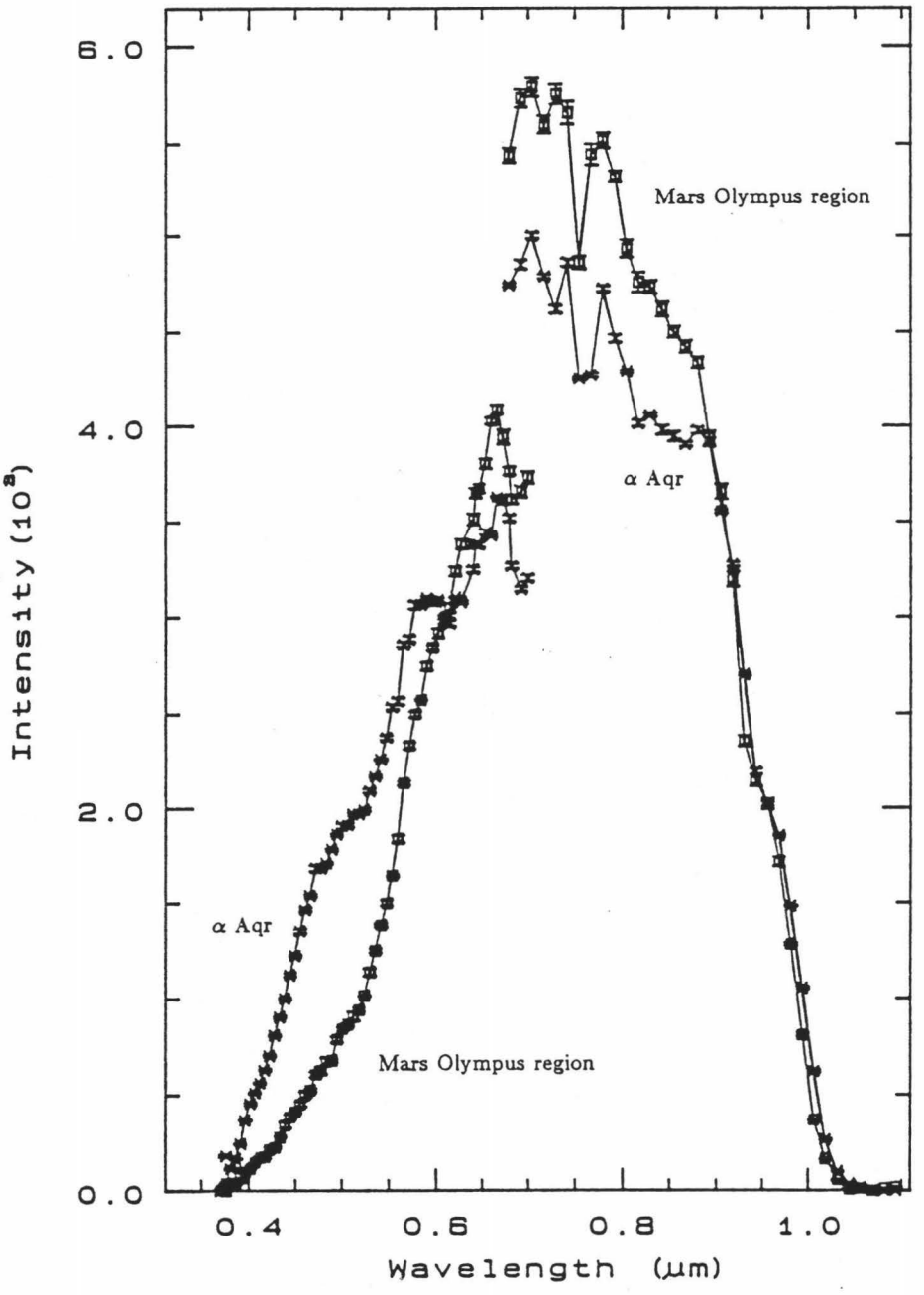

Figure 3.3. Raw flux data for the standard star α Aqr and a representative bright region on Mars (Olympus Mons, region 7 in Figure 3.2). The data were acquired with a two-segment CVF (0.37-0.713 μm and 0.679-1.094 μm, see text) and the error bars represent variation of the signal at each wavelength over a 2-3 minute period. The strong telluric Oxygen-A band at 0.76 μm is obvious in both the Mars and star data, as is the fact that Mars has a deep absorption band shortward of 0.7 μm. The signals are remarkably similar farther into the near-IR.

RESULTS AND INTERPRETATIONS

Reflectivity Spectra

Figure 3.4 shows 12 of the best scaled reflectance (Mars/16 Cyg B) spectra of the 21 obtained on the photometric evening of August 14, 1988. The spectra are divided roughly into bright, intermediate, and dark broadband albedo based on our visual monitoring of the planet during the times of observation and on telescopic albedo maps from previous oppositions (such as the Lowell Observatory map of Inge *et al.*, 1971). Many interesting results are immediately obvious in the data. First, the spectra show the strong, characteristic reflectance dropoff into the near-UV. This absorption is attributable to very intense Fe^{3+} ligand field transitions and Fe^{3+}—Fe^{3+} electronic pair transitions (Table 3.2), as well as some contribution from a strong $Fe^{3+} \rightarrow O^{2-}$ charge transfer feature at higher energies farther into the UV (Sherman and Waite 1985). This absorption is stronger in the brighter regions than in the darker regions (Figure 3.5) and seems to commence at longer wavelengths in the brighter regions. Secondly, Mars appears to be without contrast in the 0.4-0.5 μm region, although this result is somewhat clouded by very small but evident features in the near-UV which are residual absorptions in the standard star but not in the solar spectrum. This result may be due to increased Rayleigh scattering in the martian atmosphere in the near-UV which obscures surface features from view (Mars has long been known to be bland in the near-UV; this opposition shows no exception [Bell *et al.*, 1989a]) or more likely it is due to the near-saturation of the deep near-UV absorption edge. Laboratory spectra of many pure Fe^{3+}-bearing iron oxides such as hematite (αFe_2O_3) show such saturation of this absorption edge (Figure 3.6) (Sherman *et al.*, 1982; Morris *et al.*, 1985). Certainly, the band is not actually saturated in the Mars data (the longer wavelength bands would be much deeper); however, it is deep enough so that the surface materials have little or no contrast at the shorter

TABLE 3.2

Major Absorption Bands From 0.4-1.1 μm[†]

Absorber	*Spectral Region (μm)*	*Band Centers (μm)*
H_2O (vapor)	0.64-0.66	0.650
	0.70 - 0.74	0.718
	0.79 - 0.84	0.810
	0.926 - 0.978	0.935
	1.095 - 1.165	1.130
O_2	0.75-0.77	0.76
	0.68-0.70	0.69
O_3	0.44-0.75	~0.60
Fe^{3+} (Hematite)	–	~0.405
	–	~0.44
	–	0.53-0.56
	~0.6-0.7	0.64-0.65
	~0.76-0.94	0.86-0.88
Fe^{2+} (ol,px)	0.9-1.25	~1.0

[†]Gas phases from Kondratyev [1969], Fleagle and Businger [1980] and Tull [1966, fig. 2]. Fe bands from Hunt *et al.* [1971, 1973b], Sherman and Waite [1982], and Morris *et al.* [1985].

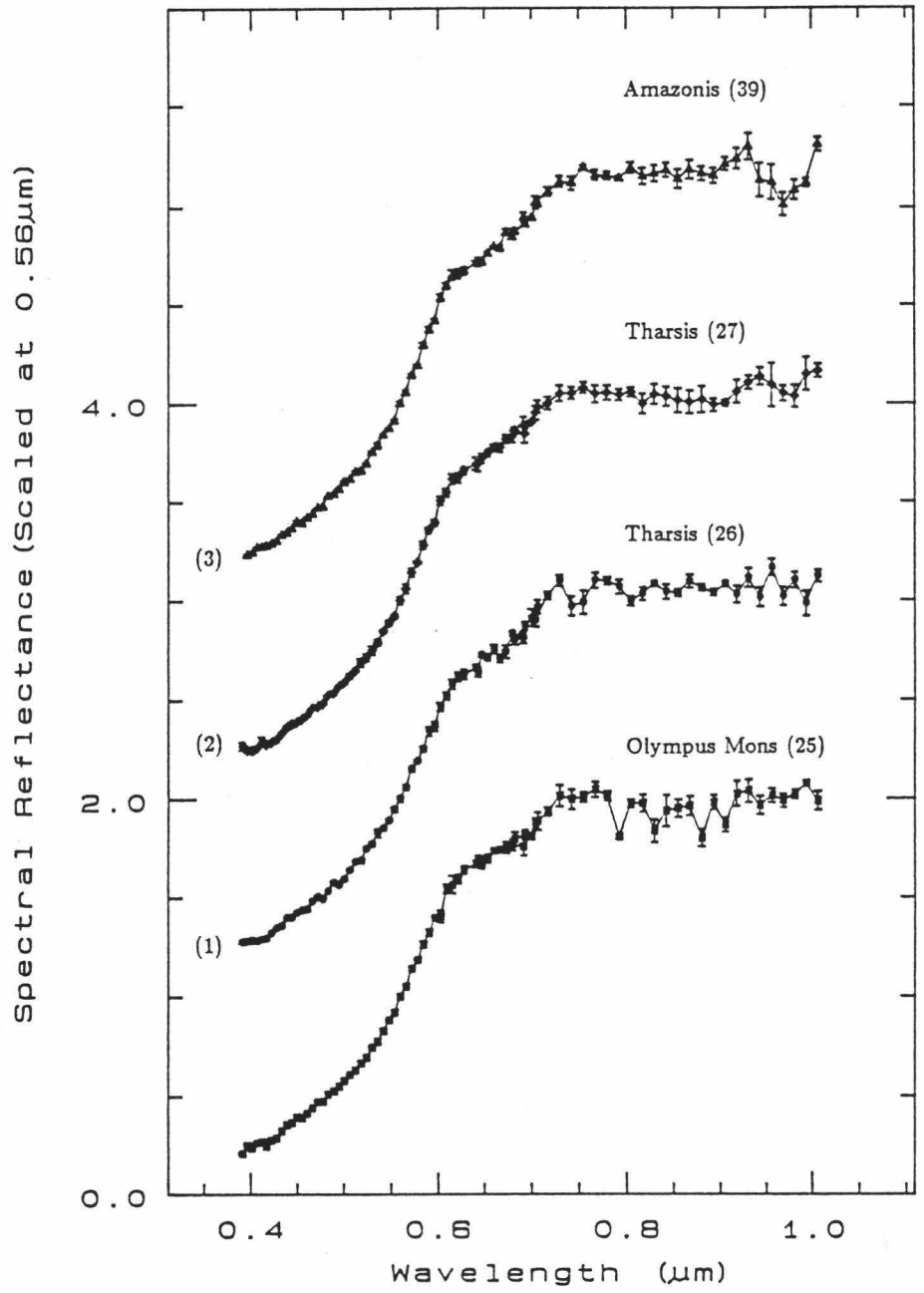

Figure 3.4.1. Approximate spectral reflectance (Mars/solar analog 16 Cyg B) for 12 regions on Mars of 500-600 km diameter. These 4 spectra (names and spot numbers correspond to Figure 3.2 and Table III-1) are some of the highest albedo regions observed based on visual monitoring at the telescope and telescopic albedo maps such as Inge *et al.* [1971]. Note the strong ~0.66 μm "cusp" in these data as well as the relative steepness of the near-UV absorption edge and the broad, very weak 0.8-0.95 μm absorption. The spectra are stacked for clarity and the offset is given to the left.

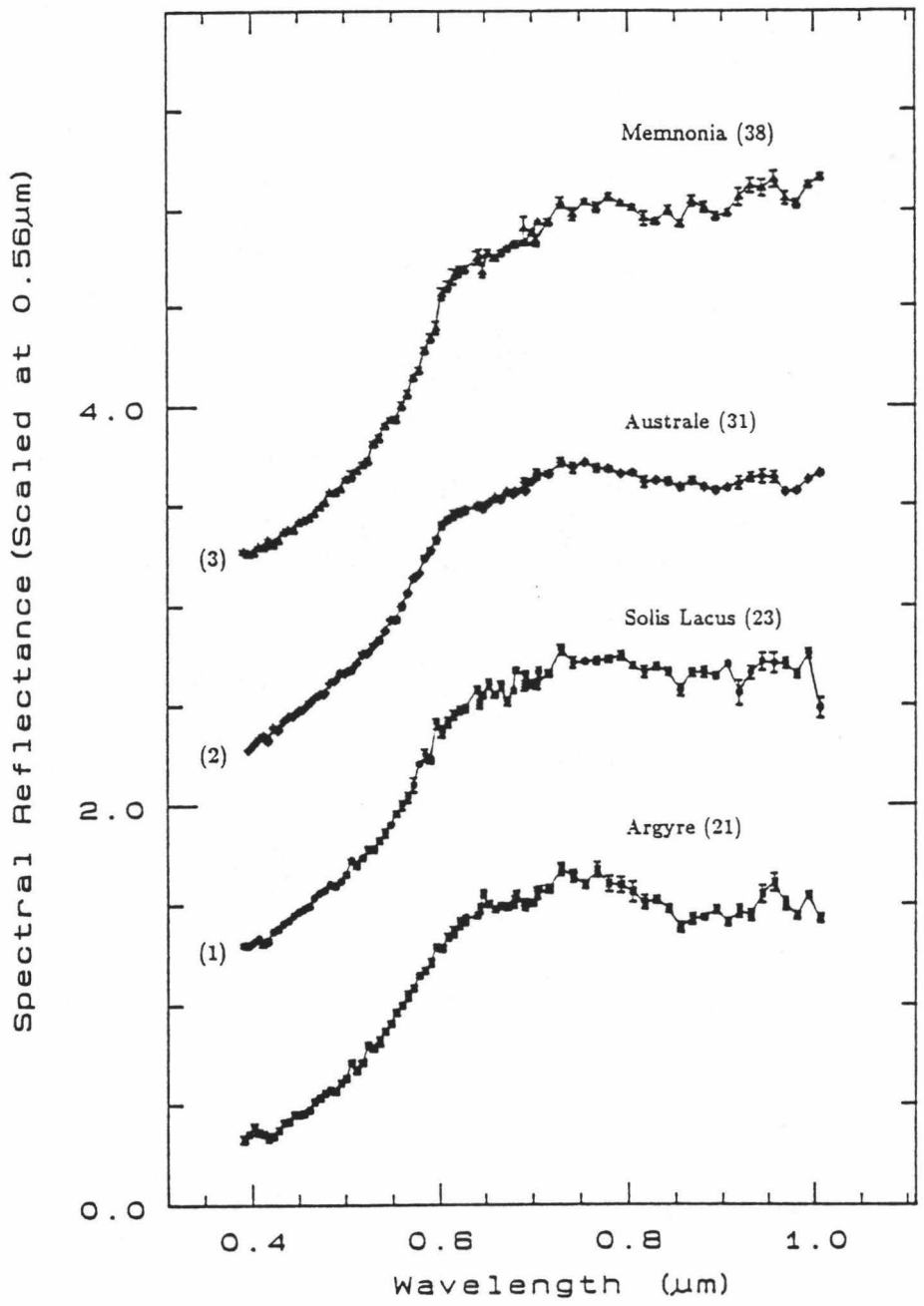

Figure 3.4.2. As in 3.4.1 except for intermediate albedo regions. The near-UV absorption edge is less steep and the ~0.66 μm "cusp" is still evident. Also, spectra of spots 21 and 31 show more evidence for the 0.81-0.94 μm absorption band.

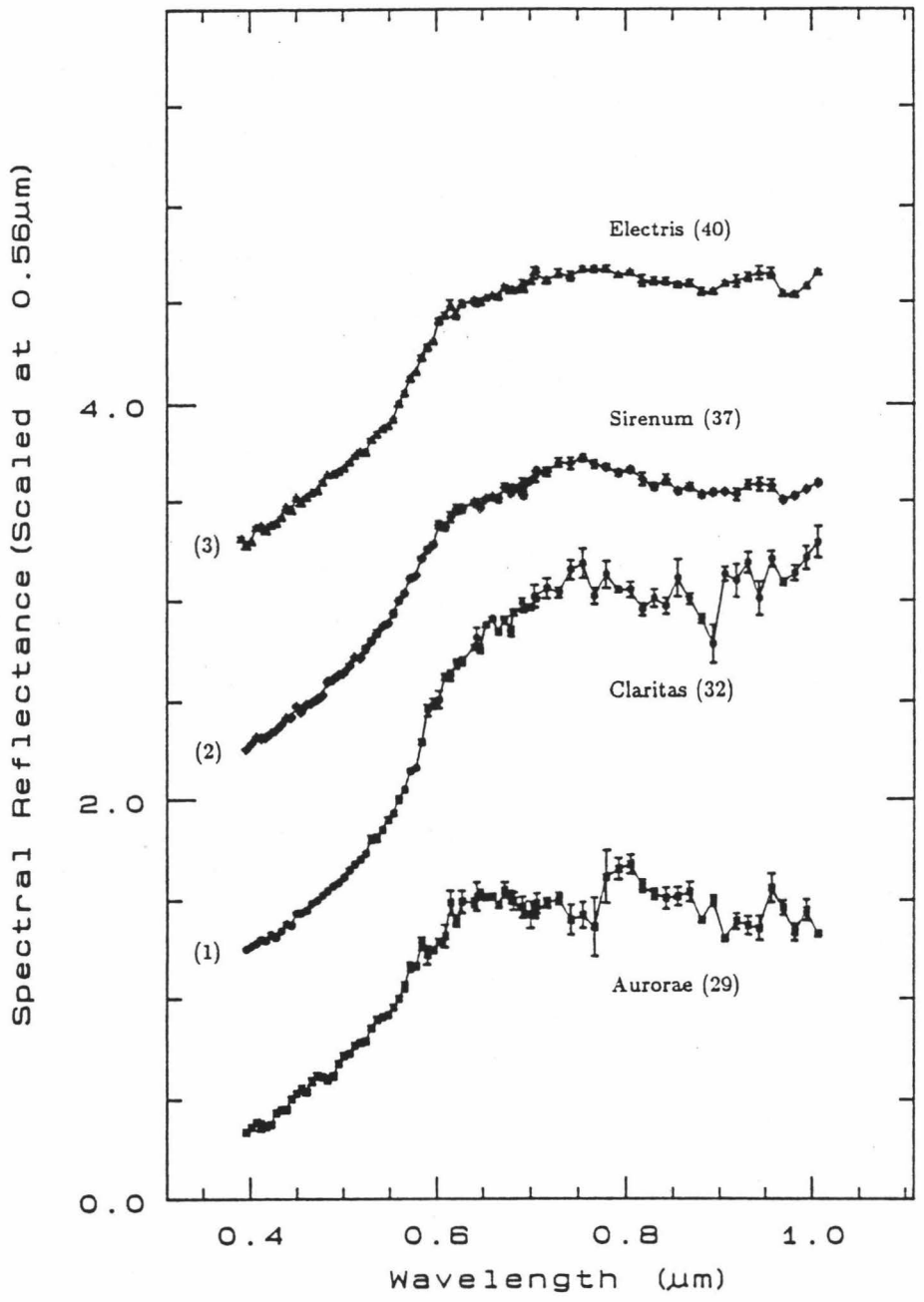

Figure 3.4.3. As in 3.4.1 except for dark albedo regions. The near-UV absorption edge is typically much less steep than in (a) and (b) (with the exception of spot 32) and the ~0.66 μm and 0.81-0.94 μm absorption bands are both evident, although spots 32 and 29 are of lower S/N.

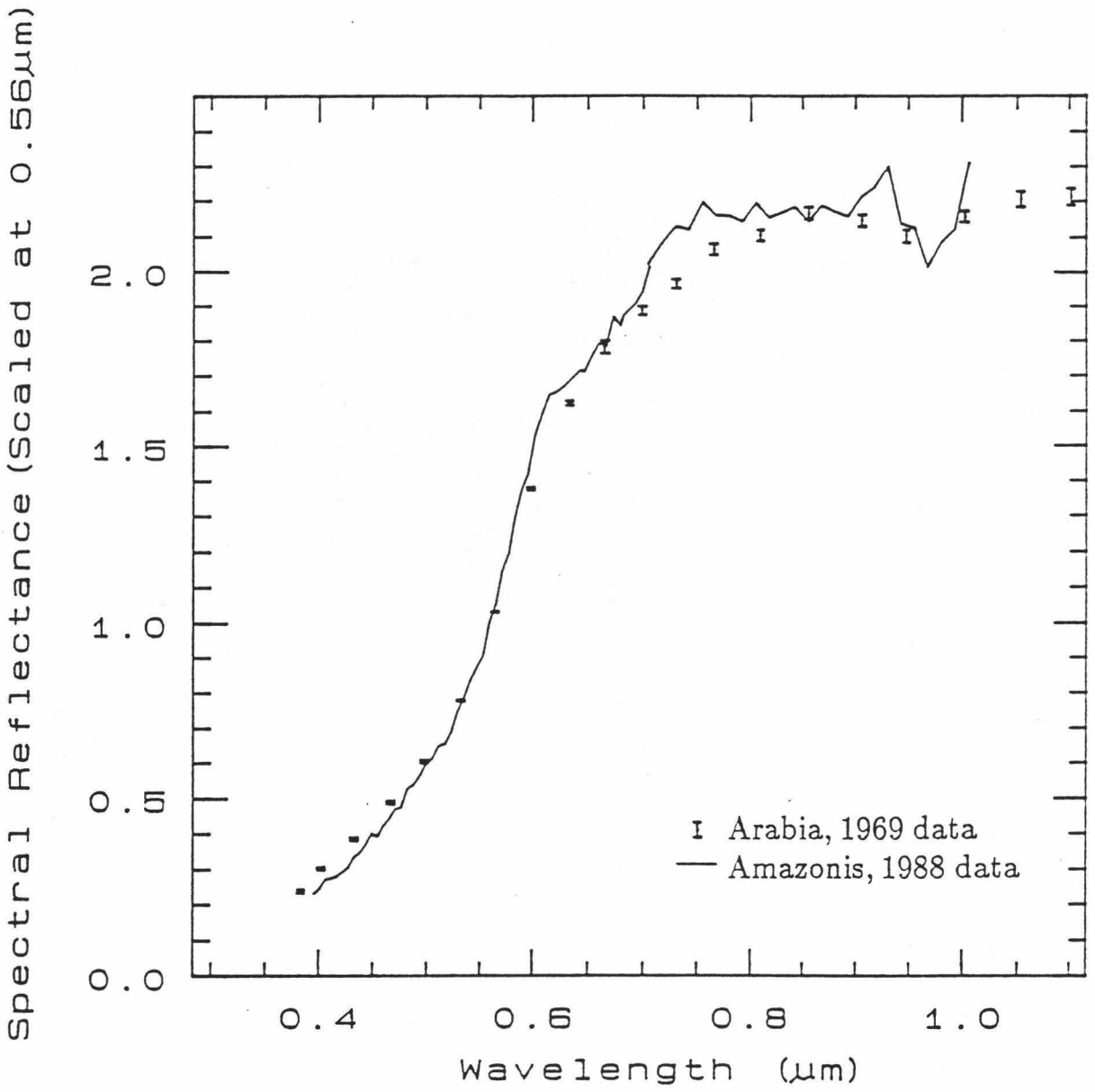

Figure 3.4.4. Spectral reflectance data for the bright region Arabia during the 1969 opposition [McCord and Westphal, 1971] compared with our data of the bright Amazonis region during the 1988 opposition. The lower resolution 1969 data show the gross spectral shape characteristic of Mars, a weak ~0.9 μm absorption, and only the slightest hint of the ~0.65 μm band so prevalent in the new, higher resolution data. The 1969 data are fairly representative of the best published data for Mars in the visible to near-IR prior to this study and played a key role in the interpretations of Morris *et al.* [1989] discussed in the text.

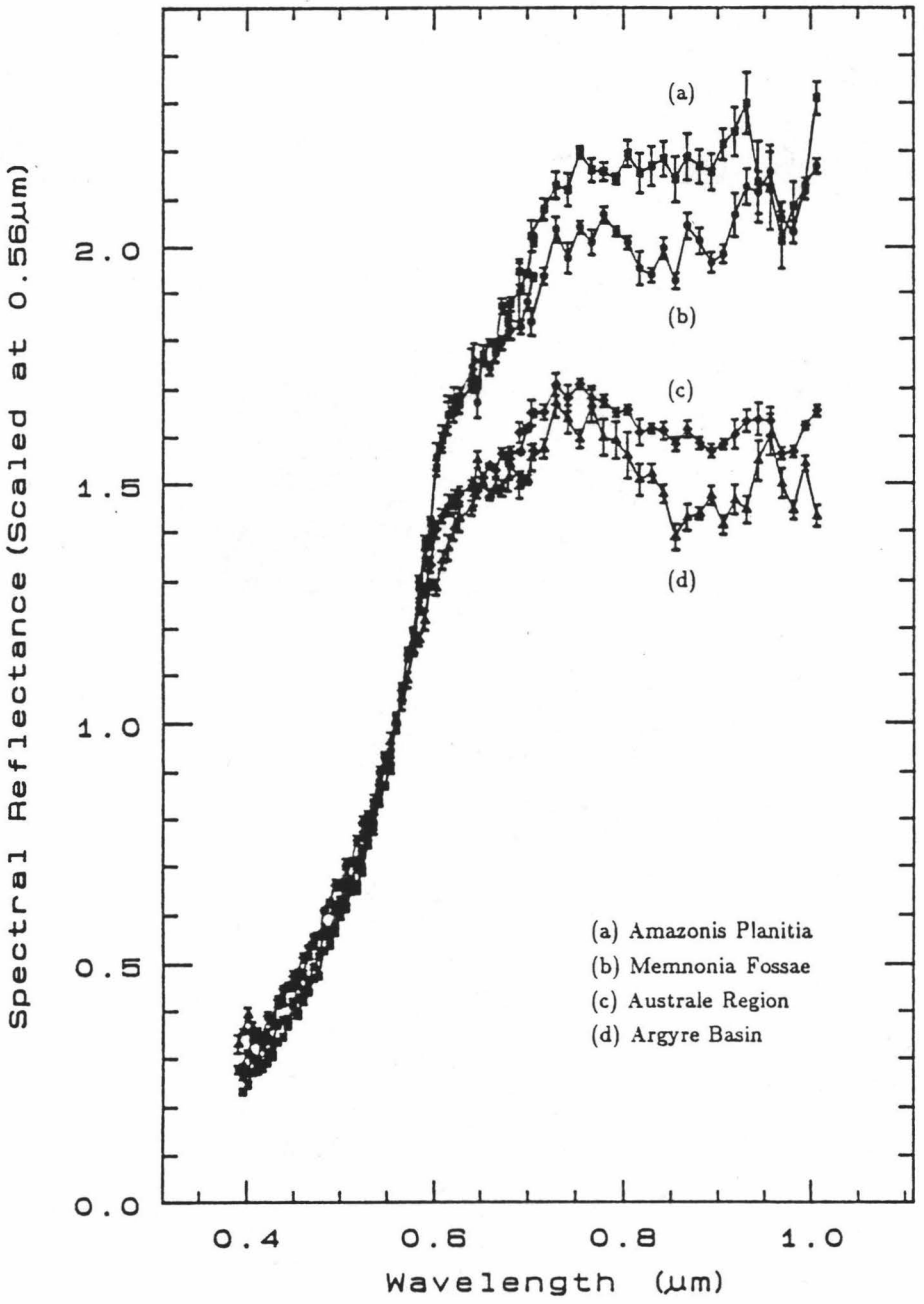

Figure 3.5. Spectra of 4 regions representing bright to dark regions which are overlayed to show how the near-UV absorption edge weakens with decreasing surface albedo. From 0.4-0.5 μm, the dark regions actually appear brighter in these scaled data than the bright regions, a fact first pointed out by actual albedo data of McCord and Westphal [1971] and possibly attributed to Rayleigh scattering or other martian atmospheric effects.

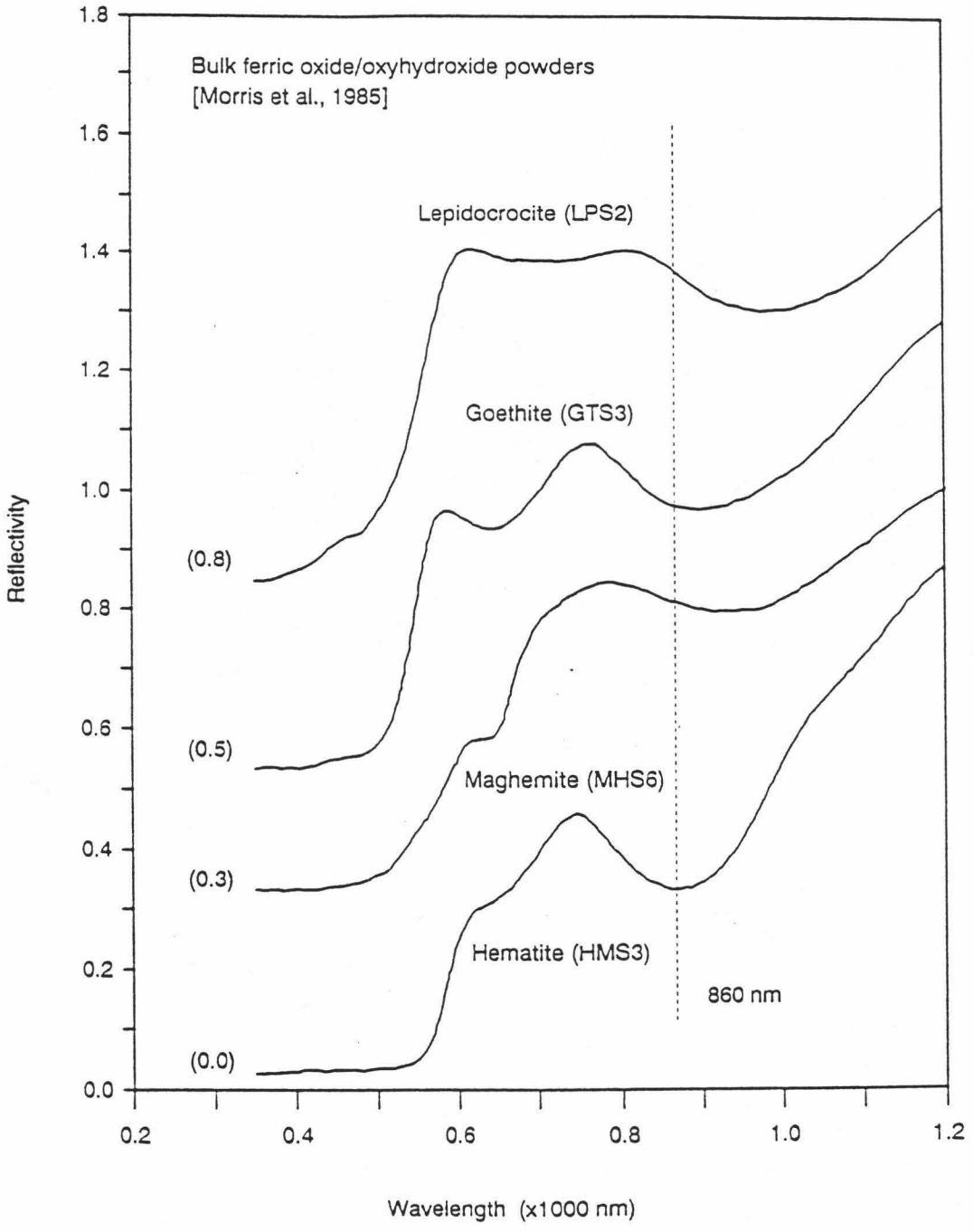

Figure 3.6. Spectra of bulk ferric oxide/oxyhydroxide powders (particle size range typically 20-1000 nm). Distinct crystalline Fe^{3+} absorption bands are seen centered at ~0.86 μm and ~0.65 μm, as is the steep near-UV absorption edge characteristic of iron oxides as well as the martian reflectance spectrum. Spectra are stacked for clarity and the offset is given to the left. Data adapted from Morris *et al.* [1985]; figure kindly provided by R.V. Morris (NASA/JSC).

wavelengths studied here. In these several respects, the spectra presented here are similar to earlier spectra of this type (*i.e.* McCord *et al.*, 1978; Singer *et al.*, 1979) which were taken at lower spectral sampling intervals and often during oppositions much less favorable than that of 1988.

Perhaps the most interesting new result evident in these data is the detection of several distinct absorption bands and inflections which have never before been as evident. Most obvious is the band or "cusp" at 0.62-0.72 μm, centered at $\sim$0.66μm, and typically deepest in spectra of brighter regions on the planet. This band is interpreted as being due to the $^6A_1 \rightarrow {}^4T_2({}^4G)$ electronic transition of Fe^{3+} located near 0.65 μm, but known to vary slightly with mineralogy (Sherman and Waite, 1985; Morris *et al.*, 1985). A second apparent band can be seen in several of the spectra in the 0.81-0.94 μm range, possibly having two band centers near 0.85 μm and 0.91 μm (the band is most obvious in spectra of spots 21, 31, and 37 in Figure 3.4). Typically, this band is strongest in the intermediate to dark albedo regions, where it is often found with the 0.66 μm band discussed previously, although this latter band is weaker in the intermediate to dark regions than in the bright regions. The 0.81-0.94 μm band is interpreted as being due to the $^6A_1 \rightarrow {}^4T_1({}^4G)$ ligand field transition of Fe^{3+} located near 0.90 μm (Sherman and Waite, 1985). The feature may also have some component due to terrestrial atmospheric water vapor bands at 0.79-0.84 μm and 0.93-0.98 μm; however, the night was photometric and humidity was low ($\sim$20%), so water vapor contamination should be minor.

It is important to point out that what are being detected in the spectra are *crystalline* absorption bands, caused, most likely, by some percentage of *crystalline* iron oxide or hydroxide in the martian surface soils and/or airborne dust. Previous data (for example McCord *et al.* 1978; Singer *et al.*, 1979) have not shown such strong evidence for crystallinity in the martian materials. There are several possible explanations for this, such as the higher spectral precision and

resolution of these measurements and the more favorable opposition in terms of proximity to Mars and lack of a global dust storm. Also, increased research into the physical and spectral properties of iron oxides as they apply to Mars by several workers in the community (Singer, 1982; Sherman *et al.*, 1982; Morris *et al.*, 1985) has allowed such interpretations to be more firmly made. Recent reinterpretations of earlier martian spectral data in the visible to near-IR by Morris *et al.* (1989) and Morris and Lauer (1989) has suggested there to be a significant component of crystalline or bulk iron oxide (most likely as hematite) in the martian surface materials based mainly on observations of a very weak 0.84-0.9 μm band seen in the martian bright region spectrum of Singer *et al.* (1979). The interpretations derived here from these much superior new data confirm the existence of that band on the surface and also show strong evidence for a second crystalline Fe^{3+} iron oxide band at 0.62-0.72 μm.

Relative Reflectance (Ratio) Spectra

Figures 3.7 and 3.8 show a number of relative reflectance spectra from August 13 and 14, 1988 data. These particular ratios were generated because of their potential of revealing absorption band or spectral slope variations between areas of different visual albedo and different geologic units (as inferred from geologic maps of Scott and Tanaka [1986] and Greeley and Guest [1987]). In general, most of the relative reflectance spectra shown in Figures 3.7 and 3.8 are featureless, exhibiting only spectral slope variations across this wavelength range. This result is consistent with the data of Chapter 2 (Bell and McCord [1989]) which indicated little spectral band variation (but definite slope and continuum variations) from 0.7-2.5 μm among similar-sized spots during the 1986 opposition in the same region of the planet studied here. Many of the features seen in the ratio spectra here are caused by variations in terrestrial atmospheric water vapor absorptions (Table 3.2), especially in Figure 3.7 which was generated from August

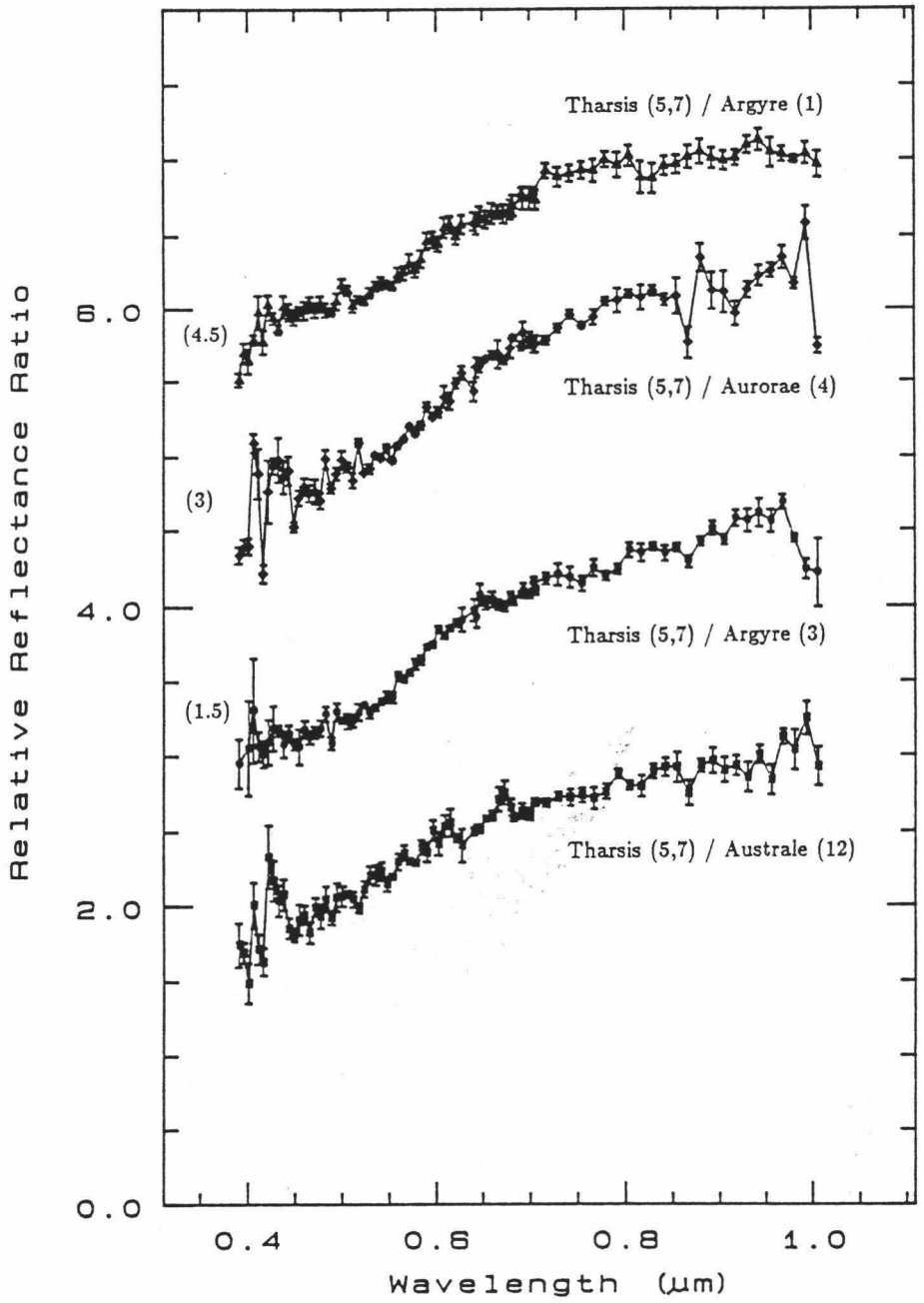

Figure 3.7.1. Relative reflectance spectra for regions on Mars observed on August 13, 1988 UT at 500-600 km resolution. These 4 spectra (names and spot numbers correspond to Figure 3.2 and Table 3.1) show variation between average bright regions (regions 5 and 7 in Tharsis) and regions of lower albedo. The bright regions are distinctly redder in color. Based on observed slope changes, it appears that the ~0.66 μm band in the bright regions is stronger than in the intermediate to dark albedo spots. The spectra are stacked for clarity and the offset is given to the left.

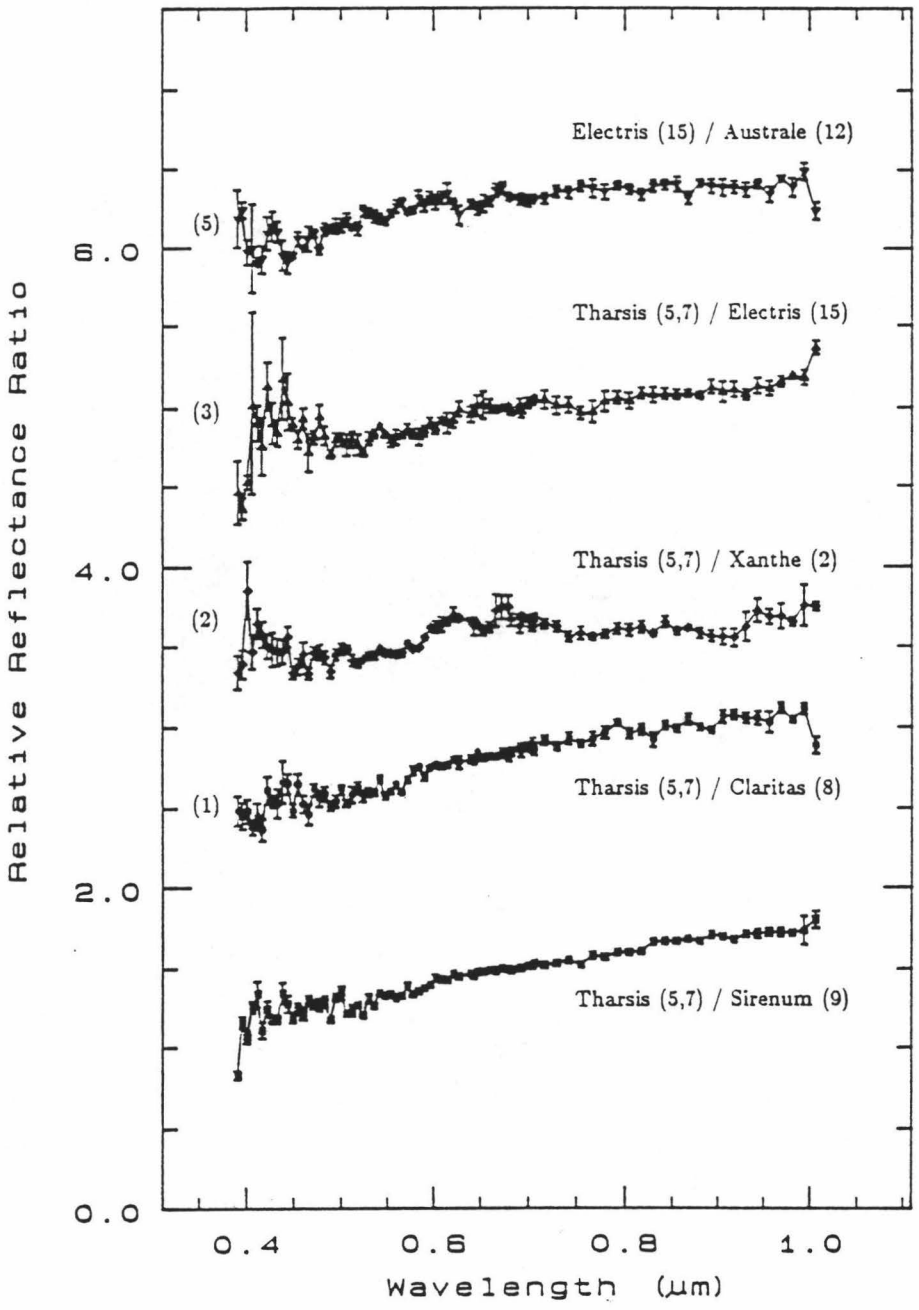

Figure 3.7.2. As in 3.7.1 except that slopes into the near-UV are less steep. The differences between the spots compared here seems to be mainly one of color, as only in the ratio of Tharsis (5,7) to Xanthe (2) is there any indication of absorption band variations.

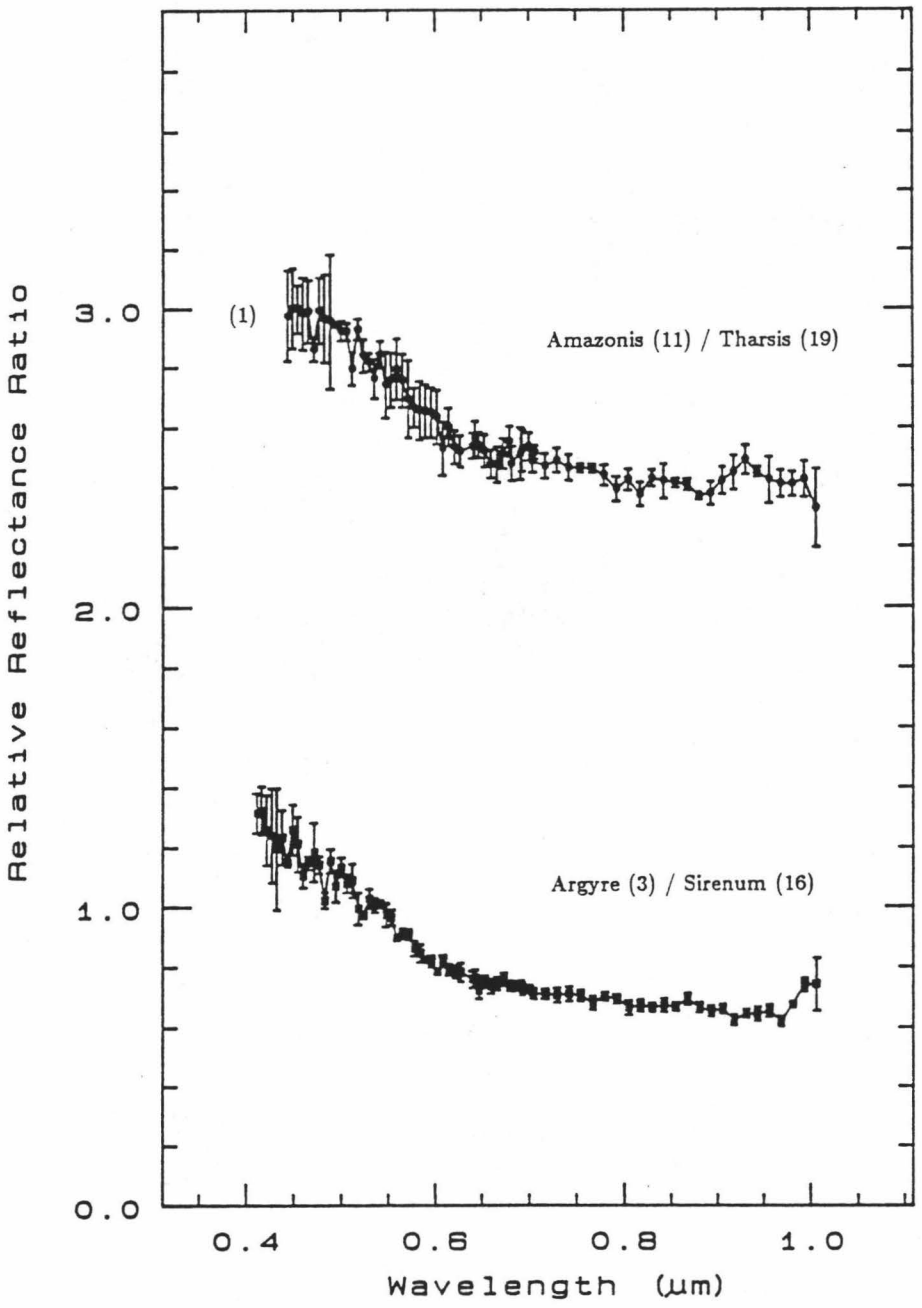

Figure 3.7.3. As in 3.7.1 except that the comparisons here are between regions of similar visual albedo. These spectra demonstrate that areas of similar brightness are not necessarily the same color. For these spectra, both Tharsis (19) and Sirenum (16) are more red than the regions to which they are compared.

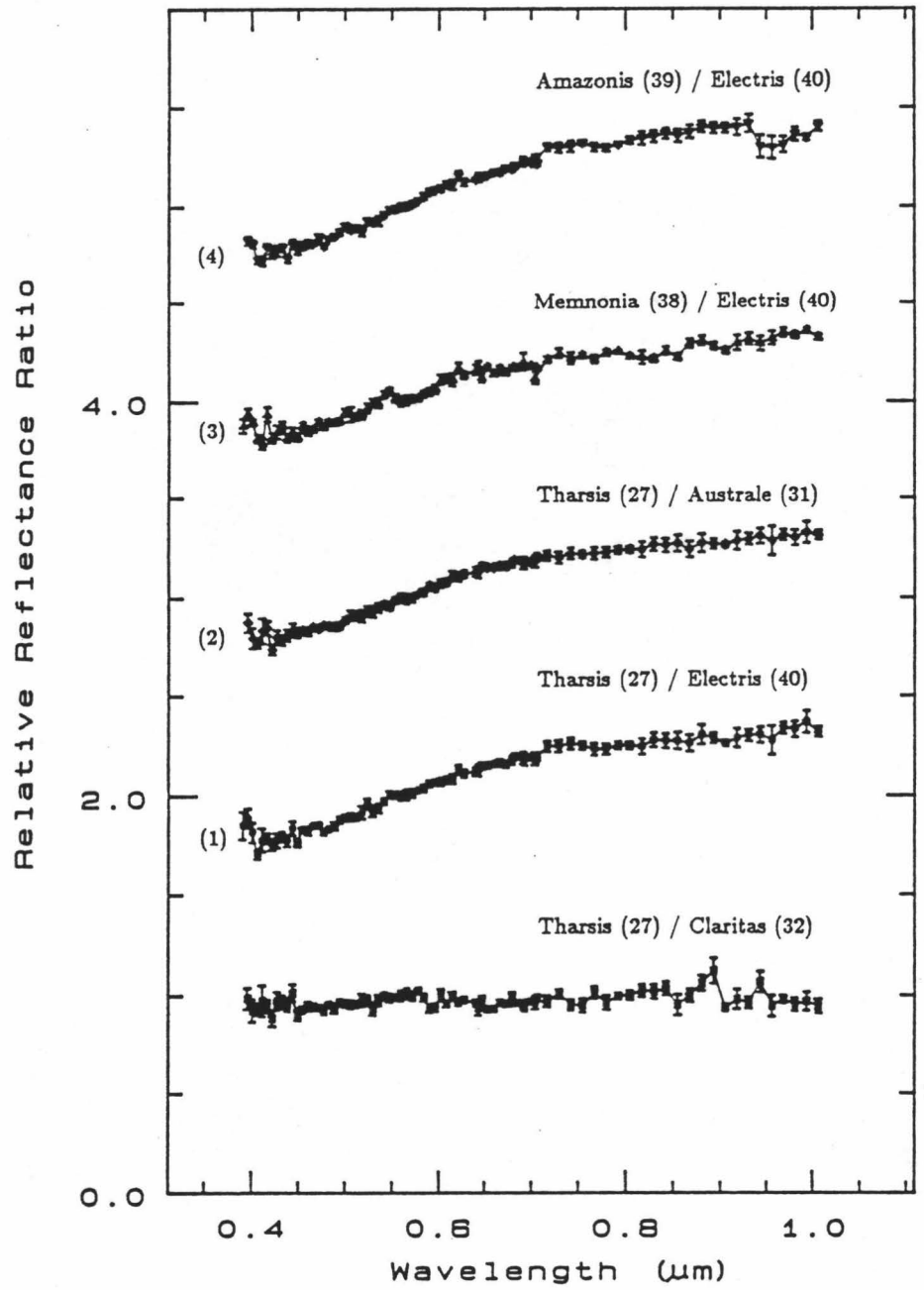

Figure 3.8.1. Relative reflectance spectra for regions on Mars observed on August 14, 1988 UT at 500-600 km resolution. These 5 spectra (names and spot numbers correspond to Figure 3.2 and Table 3.1) show broad color differences between the regions observed but little evidence for crystalline absorption band variations. The spectra are stacked for clarity and the offset is given to the left.

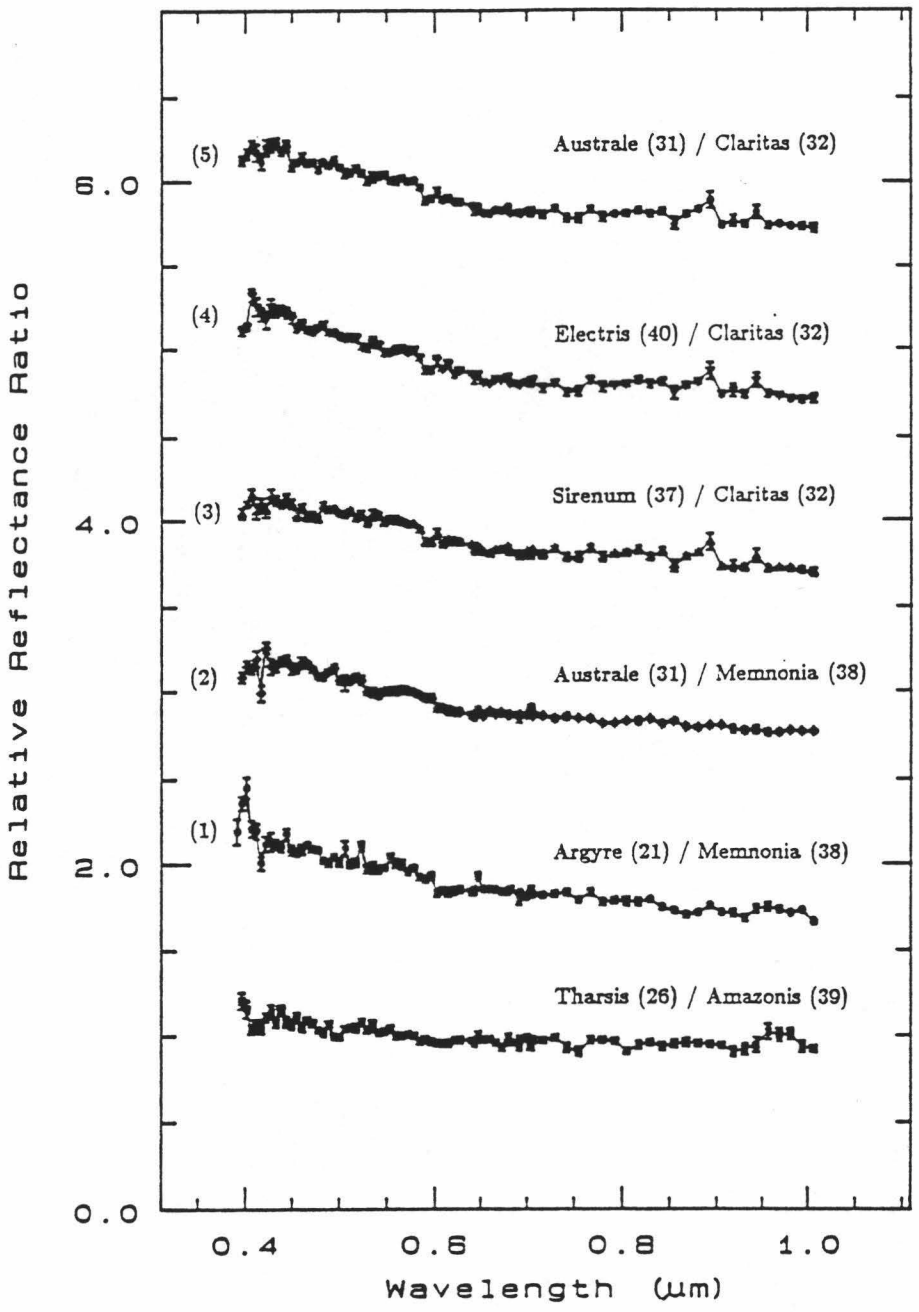

Figure 3.8.2. As in 3.8.1 except the comparisons here are between regions of similar visual albedo. Like Figure 3.7.3, this figure shows that similar brightness does not necessarily imply similar color. In general, however, regions of similar broadband albedo do not show the degree of absorption band variations seen in other relative reflectance spectra (*cf.* Figure 3.7.1).

13, 1988 non-photometric data. In a few of the ratios, such as those in Figure 3.7.1, the 0.66 μm band in the bright regions appear slightly stronger than in the intermediate and dark regions, although region 2 (Figure 3.7.2, middle ratio) in Xanthe Terra seems to exhibit a stronger 0.66 μm band than the bright Tharsis region. No variations in the ~0.81-0.94 μm band can be seen in these ratios above the noise. In general, the ratios show that the bright regions are distinctly redder than the dark or intermediate albedo regions. There appear to be distinct slope changes near 0.55, 0.6, and possibly 0.43 μm in several of the ratios which are most likely related to varying depths of the specific Fe^{3+} electronic transition bands and charge transfer features which make up the near-UV absorption edge. As well, there is a fair degree of variation in color (broadband slope) between regions of similar visual albedo (*vis.* Figures 3.7.3 and 3.8.2). Further analysis of these data will concentrate on comparison with global color units (bright red, dark red, very dark red, dark gray) determined from Viking Orbiter and Lander multispectral data (Soderblom *et al.*, 1978; Arvidson *et al.*, 1989; McEwan *et al.*, 1989). Taken together, these reflectance and relative reflectance spectra suggest, as have previous workers (*e.g.*, Adams and McCord, 1969; Huguenin *et al.*, 1977; McCord *et al.*, 1977), that the intermediate to dark albedo regions have a lower Fe^{3+} content than the bright areas of the planet.

CONCLUSIONS AND DISCUSSION

The data and interpretations of the previous section present an interesting scenario for the martian surface which must be reconciled with other work in different spectral regions. It is fairly well established on the basis of telescopic reflectance spectroscopy, Viking Orbiter Infrared Thermal Mapper (IRTM), and Viking Orbiter and Lander multispectral imaging that the bright and dark

regions of Mars represent regions of eolian dust cover accumulation and depletion, respectively (Kieffer *et al.*, 1977; Soderblom *et al.*, 1978; Singer and McCord, 1979; Palluconi and Kieffer, 1981; McCord *et al.*, 1982). The dark areas, then, represent a closer approximation to the underlying "bedrock" mineralogy of the surface than do the bright regions. The spectra in Figure 3.4 show that these dark regions generally exhibit weaker crystalline Fe^{3+} bands than the brighter regions. To some degree, this difference must be related to mineralogic differences between the bright and dark region, as discussed above. It must be noted, however, that the real spectral band differences between regions on Mars in the visible to near-IR are very small, at least at the spatial resolution of this study. This is evident from the relatively featureless relative reflectance spectra of Figures 3.7 and 3.8 (see also Chapter 2 and Bell and McCord, 1989). Although spectral differences exist between different geologic units on the surface both here and at Viking Orbiter and Lander spatial resolutions based on slope and continuum variations (Soderblom *et al.*, 1978; Evans and Adams, 1979; Guinness *et al.*, 1987; Arvidson *et al.*, 1989; McEwan *et al.*, 1989), it is unclear just how well the new groundbased data can be related to the spacecraft observations. Since the spatial resolution was so low (500-600 km), the measurements discussed here probably represent averages of units resolved at higher resolution. The main emphasis of the research presented here is on the mineralogic information contained in the reflectivity spectra.

As has been pointed out, the major implication of the spectra in Figure 3.4 is that a detectable amount of bulk, crystalline ferric oxide material exists on the surface of Mars, strengthening recent interpretations (Morris *et al.*, 1989; Morris and Lauer, 1989) based on new laboratory studies of ferric iron oxide and hydroxide minerals. In addition, this evidence of ferric iron crystallinity is consistent with the results of Guinness *et al.* (1987) who noted that palagonite-like materials do not have the steeper slopes and greater spectral curvature

necessary to explain the reflectance data of surface soils measured by the Viking Landers. Determining the exact ferric iron mineralogy is a difficult problem, however. The fact that the crystalline ferric oxide bands are weak and not easily detectable on Mars, and yet the near-UV absorption edge is deep and easily seen in even broadband data, argues that a significant part of the ferric iron mineralogy must also be in the form of amorphous or poorly crystalline palagonite-like materials (Toulmin *et al.*, 1977; Soderblom and Wenner, 1978; Gooding and Keil, 1978; Singer, 1982). There are a number of physical and geochemical difficulties with the presence of abundant palagonite or palagonite-like materials on Mars, however, which have been raised since the idea was first proposed. Specifically, recent simulations of the Viking Lander Labeled Release and Pyrolitic Release experiments (Banin and Margulies, 1983; Banin *et al.*, 1988) have shown that palagonites cannot reproduce the results of the wet chemistry experiments performed on Mars.

A more tenable solution to this problem can be found in the recent work of Morris *et al.* (1989) and Morris and Lauer (1989) on nanophase (particles $\leq$10 nm) hematites and their application to Mars spectral data. Bulk hematite, as well as other iron oxides and hydroxides, exhibits strong, distinct Fe^{3+} absorption bands in the visible to near-IR which are not evident to such a degree in the martian spectra (Figure 3.6). However, as the particle size decreases towards the nanophase materials ("crystals" of only a few unit cells), the strength of these bands decreases and the shape and position of the near-UV absorption edge more closely resembles that of the Mars data (Figure 3.9). The work of Morris *et al.* (1989) and Morris and Lauer (1989) specifically addresses the implications for hematite on Mars, and the spectral effects of nanophase particles of goethite, maghemite, magnetite, or lepidocrocite have not been studied. Thus, the presence of these other ferric oxyhydroxides cannot be entirely ruled out until further laboratory studies are undertaken. Nonetheless, it is interesting to point out that

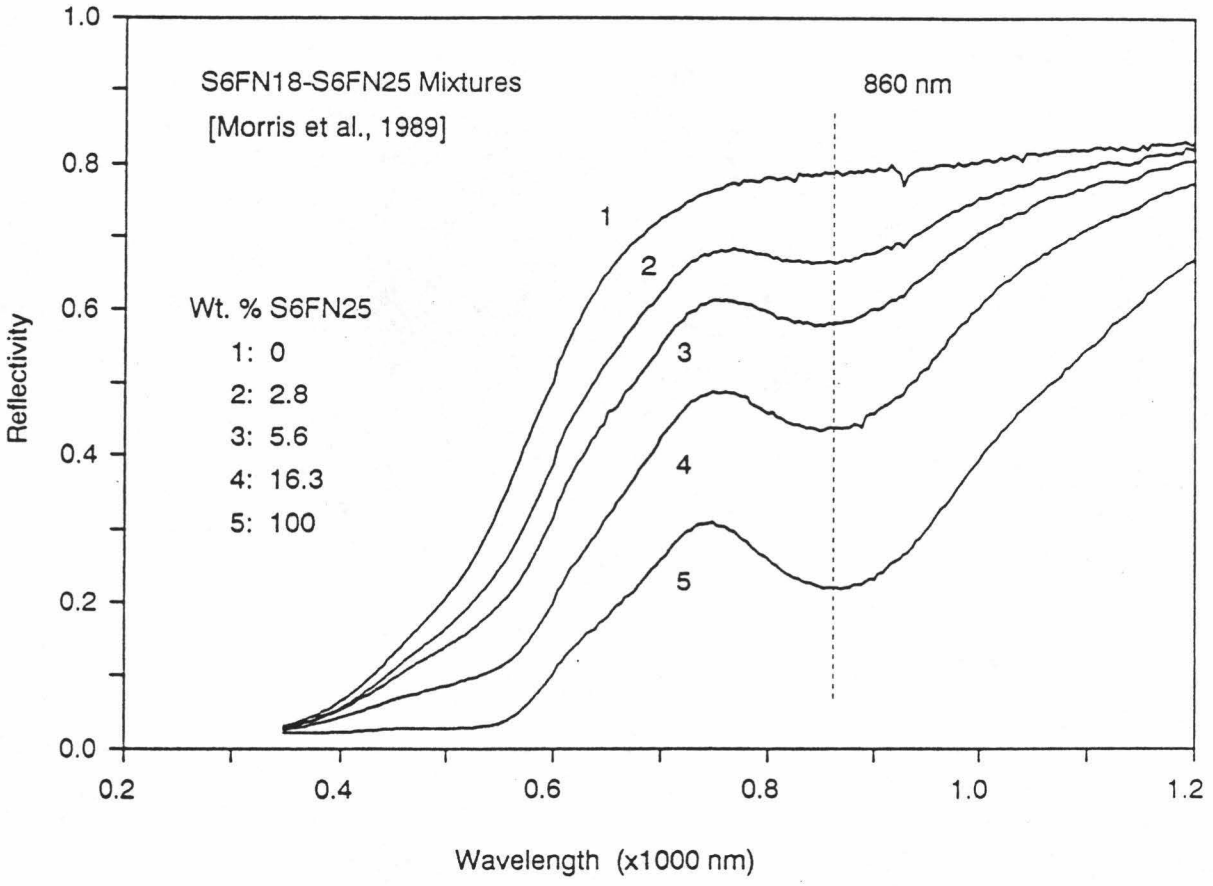

Figure 3.9. Visible to near-IR reflectance spectra of mixtures of pure nanophase hematite (sample S6FN18, Fe_2O_3 = 0.46 wt%) and pure bulk hematite (sample S6FN25, Fe_2O_3 = 19.0 wt%). Note how the spectra of nanophase hematite plus some additional bulk hematite component generally provide a good match to the martian data of Figure 3.4. Data adapted from Morris *et al.* [1989]; figure kindly provided by R.V. Morris (NASA/JSC).

the spectral data presented here *could* be explained solely by hematite as the only Fe^{3+} iron oxide on the martian surface, existing in a range of particle sizes from bulk crystals to extremely fine-grained nanophase particles.

In addition to further laboratory study of iron oxides, more study of the geochemical or chemical equilibrium stability of weathered iron oxide minerals under current martian physical conditions must be undertaken to constrain further the ferric iron mineralogy. The spectral identification of crystalline ferric oxides possibly indicates either older crustal alteration mechanisms involving higher temperatures and/or more water (Singer, 1985), or an auto-oxidation mechanism under extremely arid conditions similar to terrestrial desert environments (F. Fanale, personal communication, 1989) and thus has important implications for martian soil and rock genesis which must be examined further. Also, additional data in the 0.4-1.1 μm range were acquired during the 1988 opposition using completely different instrumentation at even higher spectral resolution (Bell *et al.*, 1989a,b). Initial analyses of these data, taken a short time after the observations described here, shows evidence of the same distinct, crystalline Fe^{3+} absorption bands seen in the data of Figure 3.4. These data are still undergoing reductions which will provide further high precision information with which to assess the ferric oxide and/or hydroxide mineralogy of the martian surface soils and airborne dust.

SUMMARY

(1) Spectral reflectance (Mars/16 Cyg B) and relative reflectance spectra have been presented for 41 predominantly western hemisphere regions on Mars obtained during the extremely favorable 1988 opposition with a circular variable filter spectrometer at Mauna Kea Observatory. The data are generally of higher

spectral resolution (R $\simeq$ 80) and higher signal-to-noise than those of previously published studies and show excellent agreement with previous work in terms of overall spectral shape.

(2) Absorption bands at 0.62-0.72 μm and 0.81-0.94 μm are unambiguously identified, which, for several regions on the planet, are stronger than any previously seen distinct surface absorption bands in this wavelength region. These bands are interpreted as Fe^{3+} electronic transition features which are indicative of *crystalline* iron oxide minerals on the martian surface.

(3) Recent work by Morris *et al.* (1985, 1989) has suggested that hematite, existing in a wide range of particle sizes from bulk crystalline size to nanophase ($\leq$10 nm), may account for nearly all of the ferric iron mineralogy on Mars based on previous spectral data of Singer *et al.* (1979). Although the existence of other nanophase iron oxides and hydroxides cannot be ruled out without further laboratory investigations, the new 1988 data presented here support the conclusion that a single iron oxide phase, most likely hematite, *could* account for all of the observed spectral behavior of the martian surface in the 0.4-1.0 μm region.

REFERENCES CITED

Adams, J.B., Lunar and martian surfaces: Petrologic significance of absorption bands in the near-infrared, *Science, 159,* 1453-1455, 1968.

Adams, J.B. and T.B. McCord, Mars: Interpretation of spectral reflectivity of light and dark regions, *J. Geophys. Res., 74,* 4851-4856, 1969.

Arvidson, R.E., E.A. Guinness, M.A. Dale-Bannister, J. Adams, M. Smith, P.R. Christensen, and R.B. Singer, Nature and Distribution of Surficial Deposits in Chryse Planitia and Vicinity, Mars, *J. Geophys. Res., 94,* 1573-1587, 1989.

Banin, A. and L. Margulies, Simulation of Viking biology experiments suggests smectites not palagonites, as martian soil analogs, *Nature, 305,* 523-525, 1983.

Banin, A., L. Margulies, and Y. Chen, Iron-montmorillonite: A spectral analog of martian soil, *Proc. Lunar Planet. Sci. Conf. 15th,* in *J. Geophys. Res., 90,* C771-C774, 1985.

Banin, A., G.C. Carle, S. Chang, L.M. Coyne, J.B. Orenberg, and T.W. Scattergood, Laboratory investigations of Mars: Chemical and spectroscopic characteristics of a suite of clays as Mars soil analogs, *Origin of Life and the Evolution of the Biosphere, 18,* 239-265, 1988.

Bell III, J.F. and T.B. McCord, Mars: Near-infrared comparative spectroscopy during the 1986 opposition, *Icarus, 77,* 21-34, 1989.

Bell III, J.F., T.B. McCord, and P.G. Lucey, Mars during the 1988 opposition: High resolution imaging and spectroscopy, *EOS, Trans. Amer. Geophys. U., 70,* 50, 1989a.

Bell III, J.F., P.G. Lucey, and T.B. McCord, High spectral resolution visible to near-IR (0.4-1.1 μm) imaging spectroscopy of Mars during the 1988 opposition, submitted to *Proc. Lunar Planet. Sci. Conf. 20th,* 1989b.

Clark, R.N., A large scale interactive one dimensional array processing system, *Publ. Astron. Soc. Pac., 92,* 221-224, 1980.

Dollfus, A., Etude des planètes par la polarisation de leur lumière, *Ann. Astrophys.,* Suppl. 4, 1957.

Eicher, D.J. and D.M. Troiani, Memories of Mars, *Astronomy, 17,* 74-79, April 1989.

Evans, D.L. and J.B. Adams, Comparison of Viking Lander multispectral images and laboratory reflectance spectra of terrestrial samples, *Proc. Lunar Planet. Sci. Conf. 10th,* 1829-1834, 1979.

Fleagle, R.G. and J.A. Businger, An Introduction to Atmospheric Physics, pp. 231-232, Academic Press, New York, 1980.

Gooding, J.L. and K. Keil, Alteration of glass as a possible source of clay minerals on Mars, *Geophys. Res. Lett., 5,* 727-730, 1978.

Greeley, R. and J.E. Guest, *Geologic Map of the Eastern Equatorial Region of*

Mars, U.S. Geological Survey, 1:15,000,000 geologic map, Map I-1802-B, 1987.

Guinness, E.A., R.E. Arvidson, M.A. Dale-Bannister, R.B. Singer, and E.A. Bruckenthal, On the spectral reflectance properties of materials exposed at the Viking landing sites, *Proc. Lunar Planet. Sci. Conf. 17th.,* in *J. Geophys. Res., 92,* E575-E587, 1987.

Hargraves, R.B., D.W. Collinson, R.E. Arvidson, and C.R. Spitzer, The Viking magnetic properties experiment: Primary mission results, *J. Geophys. Res., 82,* 4547-4558, 1977.

Hovis Jr., W.A., Infrared reflectivity of Iron Oxide Minerals, *Icarus, 4,* 425-430, 1965.

Huguenin, R.L., J.B. Adams, and T.B. McCord, Mars: Surface mineralogy from reflectance spectra, in *Lunar Science VIII,* pp. 478-480, Lunar Science Institute, Houston, 1977.

Hunt, G.R., L.M. Logan, and J.W. Salisbury, Mars: Components of infrared spectra and composition of the dust cloud, *Icarus, 18,* 459-469, 1973a.

Hunt, G.R., J.W. Salisbury, and C.J. Lenhoff, Visible and near-infrared spectra of minerals and rocks. III. Oxides and hydroxides, *Mod. Geol., 2,* 195-205, 1971.

Hunt, G.R., J.W. Salisbury, and C.J. Lenhoff, Visible and near-infrared spectra of minerals and rocks. VI. Additional silicates, *Mod. Geol., 4,* 85-106, 1973b.

Inge, J.L., C.F. Capen, L.J. Martin, and B.Q. Faure, Mars—1969, albedo map, Lowell Obs. Map Series, 1971.

Kieffer, H.H., T.Z. Martin, A.R. Peterfreund, B.M. Jakosky, E.D. Miner, and F.D. Palluconi, Thermal and albedo mapping of Mars during the Viking primary mission, *J. Geophys. Res., 82,* 4249-4292, 1977.

Kondratyev, K.Y., Radiation in the Atmosphere, pp. 107-139, International Geophysics Series Vol. 12, Academic Press, New York, 1969.

McCord, T.B. and J.B. Adams, Spectral reflectivity of Mars, *Science, 163* 1058-1060, 1969.

McCord, T.B. and J.A. Westphal, Mars: Narrow-band photometry, from 0.3 to 2.5 microns, of surface regions during the 1969 apparition, *Astrophys. J., 168,* 141-153, 1971.

McCord, T.B., J.H. Elias, and J.A. Westphal, Mars: The spectral albedo (0.3-2.5 μm) of small bright and dark regions, *Icarus, 14,* 245-251, 1971.

McCord, T.B., R.L. Huguenin, D. Mink, and C. Pieters, Spectral reflectance of martian areas during the 1973 opposition: Photoelectric filter photometry 0.33-1.10 μm, *Icarus, 31,* 25-39, 1977.

McCord, T.B., R.N. Clark, and R.L. Huguenin, Mars: Near-infrared spectral reflectance and compositional implication, *J. Geophys. Res., 83,* 5433-5441, 1978.

McCord, T.B., R.B. Singer, B.R. Hawke, J.B. Adams, D.L. Evans, J.W. Head, P.J. Mouginis-Mark, C.M. Pieters, R.L. Huguenin, and S.H. Zisk, Mars: Definition and characterization of global surface units with emphasis on composition, *J. Geophys. Res., 87,* 10129-10148, 1982.

McEwan, A.S., L.A. Soderblom, J.D. Swann, and T.L. Becker, Mars' global color and albedo (abstract), in *Lunar and Planetary Science Conference XX,* pp. 660-661, Lunar and Planetary Institute, Houston TX, 1989.

Morris, R.V. and H.V. Lauer Jr., Matrix effects for reflectivity spectra of dispersed nanophase (superparamagnetic) hematite with application to martian spectral data, submitted to *J. Geophys. Res.,* 1989.

Morris, R.V. and S.C. Neely, Diffuse reflectance spectra of pigmentary-sized iron oxides, iron oxyhydroxides, and their mixtures: Implications for the reflectance spectra of Mars (abstract), in *Lunar and Planetary Science XII,* pp. 723-725, The Lunar and Planetary Institute, Houston, 1981.

Morris, R.V., H.V. Lauer Jr., C.A. Lawson, E.K. Gibson Jr., G.A. Nace, and C. Stewart, Spectral and other physicochemical properties of submicron powders of hematite ($\alpha-Fe_2O_3$), maghemite ($\gamma-Fe_2O_3$), magnetite (Fe_3O_4), goethite ($\alpha-FeOOH$), and lepidocrocite ($\gamma-FeOOH$), *J. Geophys. Res., 90,* 3126-3144, 1985.

Morris, R.V., D.G. Agresti, H.V. Lauer Jr., J.A. Newcomb, T.D. Shelfer, and A.V. Murali, Evidence for pigmentary hematite on Mars based on optical, magnetic, and Mossbauer studies of superparamagnetic (nanocrystalline) hematite, *J. Geophys. Res., 94,* 2760-2778, 1989.

Palluconi, F.D. and H.H. Kieffer, Thermal inertia mapping of Mars from 60 ° S to 60 ° N, *Icarus, 45,* 415-426, 1981.

Pollack, J.B. and C. Sagan, An analysis of martian photometry and polarimetry, *Smithsonian Astrophys. Obs. Spec. Rept., 258,* 1967.

Sagan, C., J.P. Phaneuf, and M. Ihnat, Total reflection spectrophotometry and thermogravimetric analysis of simulated martian surface materials, *Icarus, 4,* 43-61, 1965.

Scott, D.H. and K.L. Tanaka, *Geologic Map of the Western Equatorial Region of Mars,* U.S. Geological Survey, 1:15,000,000 geologic map, Map I-1802-A, 1986.

Sharanov, V.V., A lithological interpretation of the photometric and colorimetric studies of Mars, *Soviet Astron.—AJ., 5,* 199-202, 1961.

Sherman, D.M. and T.D. Waite, Electronic spectra of Fe^{3+} oxides and oxide hydroxides in the near IR to near UV, *Amer. Min., 70,* 1262-1269, 1985.

Sherman, D.M., R.G. Burns, and V.M. Burns, Spectral characteristics of the iron oxides with application to the martian bright region mineralogy, *J. Geophys. Res., 87,* 10169-10180, 1982.

Singer, R.B., Spectral evidence for the mineralogy of high albedo soils and dust on Mars, *J. Geophys. Res., 87,* 10159-10168, 1982.

Singer, R.B., Spectroscopic observations of Mars, *Adv. Space Res., 5,* 59-68, 1985.

Singer, R.B. and T.B. McCord, Mars: Large scale mixing of bright and dark surface materials and implications for analysis of spectral reflectance, *Proc. Lunar Planet. Sci. Conf. 10th,* 1835-1848, 1979.

Singer, R.B., T.B. McCord, R.N. Clark, J.B. Adams, and R.L. Huguenin, Mars surface composition from reflectance spectroscopy: A summary, *J. Geophys. Res., 84,* 8415-8426, 1979.

Soderblom, L.A. and D.B. Wenner, Possible fossil H_2O liquid-ice interfaces in the martian crust, *Icarus, 34,* 622-637, 1978.

Soderblom, L.A., K. Edward, E.M. Eliason, E.M. Sanchez, and M.P. Charette, Global color variations on the martian surface, *Icarus, 34,* 444-464, 1978.

Toulmin III, P., A.K. Baird, B.C. Clark, K. Keil, H.J. Rose Jr., R.P. Christian, P.H. Evans, and W.C. Kelliher, Geochemical and Mineralogical Interpretation of the Viking inorganic chemical results, *J. Geophys. Res., 82,* 4625-4634, 1977.

Tull, R.G., The reflectivity spectrum of Mars in the near-infrared, *Icarus, 5,* 505-514, 1966.

de Vaucouleurs, G., Geometric and photometric parameters of the terrestrial planets, *Icarus, 3,* 187-235, 1964.

Younkin, R.L., A search for Limonite near-infrared spectral features on Mars, *Astrophys. J., 144,* 809-818, 1966.

CHAPTER 4

SUMMARY AND CONCLUSIONS

This thesis has presented the results of three years of telescopic observations of Mars and subsequent data reduction. The data have been acquired through separate instruments in the 0.7-2.5 μm (Chapter 2) and 0.4-1.0 μm (Chapter 3) wavelength regions. Each of these studies was tailored to address a specific problem in martian surface mineralogy. The results of these two seemingly independent projects can be synthesized, however, to yield some interesting insights into the physical, chemical, and mineralogic state of the surface of Mars both currently and during its long evolution.

The basic result of the observations in Chapter 2 is that the spectral differences are small (only a few percent of the continuum) or nonexistent among many areas of Mars on the scale of several hundred kilometers. The most likely cause of this observation is that a grossly uniform mantle of global dust blankets much of the surface. Specific mineralogic information about the dust mantle was not obtained during the 1986 opposition, however. Thus there was widespread agreement that the dust mantle represented eolian transported weathering products, but little direct information on the mineralogy of the surface which would be needed to more rigorously determine the nature of the surface/atmospheric weathering processes.

Chapter 3 has presented some new mineralogic information with which to further address this issue. Spectra collected during the 1988 opposition showed absorption bands interpreted as Fe^{3+} electronic transition features indicative of crystalline iron oxide minerals on the martian surface. The specific strengths and positions of these bands, when compared with terrestrial laboratory studies, led to

the further suggestion that *at least* hematite (αFe_2O_3), existing in a wide range of particle sizes from bulk crystalline sizes to nanophase ($\leq$10 nm) occurs on Mars. The existence of other iron oxides or hydroxides could not be unambiguously ruled out from these data.

This thesis research has concentrated mainly on data acquisition and reduction, and only partly on interpretations. This has been necessarily the case, since (a) prior to this work little high quality, high spectral resolution (by telescopic standards) data had existed for Mars in the visible to near-IR and (b) laboratory studies of iron oxides and hydroxides, specifically in terms of nanophase materials, are incomplete. The stage has thus been set for future directions that this research will take. Further laboratory studies of the complete suite of iron oxides and hydroxides (*e.g.*, hematite, goethite, lepidocrocite, maghemite) in terms of spectral effects of grain size and degree of crystallinity will provide a more complete and detailed understanding of these potential Mars soil analog materials. The ultimate goal and use of the data presented in this thesis research is to identify the surface iron mineralogy of Mars. Once this is achieved, or at least once the problem is better constrained than it is today, viable scenarios for the past physical and chemical evolution of the planet can be formulated based on comparison with terrestrial weathering scenarios and projected weathering conditions on the martian surface both past and present. For the first time since intensive, focused studies of Mars began more than 100 years ago, the data exist which may finally provide an unambiguous solution to this enigmatic problem.